J Am Soc Nephrol. 2021 Jun; 32(6): 1389–1408. PMCID: PMC8259650
Published online 2021 Jun 1. doi: 10.1681/ASN.2020081213: 10.1681/ASN.2020081213 PMID: 33785583

ADAM10-Mediated Ectodomain Shedding Is an Essential Driver of Podocyte Damage

Marlies Sachs, [1] Sebastian Wetzel, [2] Julia Reichelt, [1] Wiebke Sachs, [1] Lisa Schebsdat, [1] Stephanie Zielinski, [1] Lisa Seipold, [2] Lukas Heintz, [1] Stephan A. Müller, [3,4] Oliver Kretz, [6] Maja Lindenmeyer, [6] Thorsten Wiech, [7] Tobias B. Huber, [6] Renate Lüllmann-Rauch, [8] Stefan F. Lichtenthaler, [3,4,5] Paul Saftig,[2] and Catherine Meyer-Schwesinger[1]

[1]Institute of Cellular and Integrative Physiology, University Medical Center Hamburg-Eppendorf, Hamburg, Germany
[2]Institute of Biochemistry, Christian-Albrechts University Kiel, Kiel, Germany
[3]German Center for Neurodegenerative Diseases (DZNE), Munich, Germany
[4]Neuroproteomics, School of Medicine, University Hospital rechts der Isar, Technical University of Munich, Munich, Germany
[5]Munich Cluster for Systems Neurology (SyNergy), Munich, Germany
[6]III. Department of Medicine, University Medical Center Hamburg-Eppendorf, Hamburg, Germany
[7]Nephropathology, University Medical Center Hamburg-Eppendorf, Hamburg, Germany
[8]Institute of Anatomy, Christian-Albrechts University Kiel, Kiel, Germany
Corresponding author.
Correspondence: Dr. Paul Saftig, Institute of Biochemistry, Christian-Albrechts University Kiel, Kiel, Germany, or Prof. Catherine Meyer-Schwesinger, Institute of Cellular and Integrative Physiology, University Medical Center Hamburg-Eppendorf, Hamburg, Germany. E-mail: psaftig@biochem.uni-kiel.de or c.meyer-schwesinger@uke.uni-hamburg.de
M.S., S.W., P.S., and C.M.-S. contributed equally to this work.

Received 2020 Aug 23; Accepted 2021 Feb 8.

Significance Statement

Podocytes interdigitate, forming the renal blood filter through a modified adherens junction, the slit diaphragm. Loss of podocytes due to injury could be mediated by the cleavage of podocyte cell-adhesion molecules through the action of the ectodomain sheddase A Disintegrin and Metalloproteinase 10 (ADAM10). ADAM10 is highly abundant at the site of blood filtration, the podocyte foot processes. Podocyte-expressed ADAM10 is not required for the development of the renal filter, but plays a major role in podocyte injury. After antibody-mediated injury, ADAM10 is upregulated in humans and mice. The protein cleaves cell-adhesion molecules at the

slit diaphragm, leading to Wnt/β-catenin signaling and podocyte loss. Therefore, ADAM10-mediated ectodomain shedding of injury-related cadherins drives podocyte injury.

Keywords: proteinuria, podocyte, glomerular disease, membranous nephropathy

Visual Abstract

Keywords: proteinuria, podocyte, glomerular disease, membranous nephropathy

Abstract

Background

Podocytes embrace the glomerular capillaries with foot processes, which are interconnected by a specialized adherens junction to ultimately form the filtration barrier. Altered adhesion and loss are common features of podocyte injury, which could be mediated by shedding of cell-adhesion molecules through the regulated activity of cell surface–expressed proteases. A Disintegrin and Metalloproteinase 10 (ADAM10) is such a protease known to mediate ectodomain shedding of adhesion molecules, among others. Here we evaluate the involvement of ADAM10 in the process of antibody-induced podocyte injury.

Methods

Membrane proteomics, immunoblotting, high-resolution microscopy, and immunogold electron microscopy were used to analyze human and murine podocyte ADAM10 expression in health and kidney injury. The functionality of ADAM10 ectodomain shedding for podocyte development and injury was analyzed, *in vitro* and *in vivo*, in the anti-podocyte nephritis (APN) model in podocyte-specific, ADAM10-deficient mice.

Results

ADAM10 is selectively localized at foot processes of murine podocytes and its expression is dispensable for podocyte development. Podocyte ADAM10 expression is induced in the setting of antibody-mediated injury in humans and mice. Podocyte ADAM10 deficiency attenuates the clinical course of APN and preserves the morphologic integrity of podocytes, despite subepithelial immune-deposit formation. Functionally, ADAM10-related ectodomain shedding results in cleavage of the cell-adhesion proteins N- and P-cadherin, thus decreasing their injury-related surface levels. This favors podocyte loss and the activation of downstream signaling events through the Wnt signaling pathway in an ADAM10-dependent manner.

Conclusions

ADAM10-mediated ectodomain shedding of injury-related cadherins drives podocyte injury.

The complexly structured glomerular filtration barrier (GFB) of the kidney enables size and charge selection. The GFB consists of the endothelial cell layer; the glomerular basement membrane (GBM); and the slit diaphragm (SD), a specialized adherens junction interconnecting podocyte foot processes (FPs).[1,2] Podocytes are an elementary component of the filtration barrier, because podocyte injury or apoptosis hampers filtration-barrier functions.[3,4] Podocyte injury can be induced by autoantibodies that bind to the extracellular domain of FP proteins located at the FP plasma membrane. As a result, subepithelial deposits composed of antigen-antibody complexes are formed, along with exogenous nonpodocyte proteins, such as complement components.[5] In this process, cell-surface adhesion protein contacts can be damaged or modulated; this affects podocyte cell adhesion but also the organization of FP morphology and reduces their interdigitation—a process termed podocyte FP effacement (FPE).[6] FPE impairs the organization and integrity of the SD and, consequently, normal filtration functioning.[7] Once the structure of the filtration barrier is impaired, massive proteinuria develops and this causes concomitant hypoproteinemia and ascites, which are classic symptoms of nephrotic syndrome.

Knowledge of the pathophysiologic processes underlying antibody-mediated podocyte injury are mainly based on studies in the rat Heymann nephritis model.[8] Because one of the major target proteins in Heymann nephritis, megalin,[9] is not expressed in human podocytes, further models have been developed to address the processes of antibody-induced podocyte injury. The recently developed, antigen-specific models of THSD7A or phospholipase A2 receptor 1 (PLA_2R1) autoantibody–associated podocyte injury are only functional in BALB/c mice.[10,11] Therefore, the murine anti-podocyte nephritis (APN) model emerged as an elegant method due to the effective and low-invasive induction of immune deposits in the glomeruli of C57BL/6 mice.[12,13] Anti-podocyte antibodies are injected into mice and then bind to podocyte proteins, resulting in podocyte injury characterized by subepithelial deposits, FPE, podocyte loss, and the development of a severe nephrotic syndrome.

The tight adhesion of cells can be loosened by the regulated activity of cell surface–expressed proteases that mediate the shedding of cell-adhesion molecules. A Disintegrin and Metalloproteinase 10 (ADAM10) is such a critical surface-expressed protease that mediates ectodomain shedding of substrates, such as adhesion molecules of the cadherin family and the Notch receptor.[14–17] ADAM10-dependent cleavage of the Notch receptor initiates Notch signaling, which is an important developmental regulator in kidney and other tissues.[18] In the context of podocyte injury, Notch activity was demonstrated to drive podocyte apoptosis, thereby promoting glomerulosclerosis and filtration impairment.[19] Additionally, shedding of cadherins not only affects cell adhesion and migration, but also promotes Wnt signaling through release of carboxy-terminal (C-terminal) membrane–bound β-catenin,[14,15] a pathway which, in turn, drives podocyte injury.[20] Consequently, ADAM10-mediated cleavage of cadherins directly regulates β-catenin signaling.[14] Here, we elucidate the possible role of ADAM10-mediated ectodomain shedding in antibody-mediated podocyte injury.

Methods

Antibodies

The following antibodies were used for the study: rat anti-ADAM10 (IF human and naive mice, 1:100; immunogold electron microscopy [EM], 1:25; mAb946 R&D Systems), rabbit anti-ADAM10 (IF human and diseased mice, 1:100; WB, 1:1000; Abcam), rabbit anti-ADAM10 (IF diseased mice, 1:100; WB, 1:1000; Pineda), rabbit anti-ADAM10 (IF diseased mice, 1:100; WB, 1:1000; GTX63486 GenTex), rabbit anti–N-cadherin (WB, 1:1000; IF, 1:200; Abcam), mouse anti–N-cadherin (IF cells, 1:100; 610921BD Bioscience), rabbit anti–P-cadherin (IF, 1:100; bs-1159r Bioss), rabbit anti–β-catenin (WB, 1:1000; IF, 1:100; Cell Signaling), rabbit anti–phospho-β-catenin (WB, 1:1000; IF, 1:100; Millipore), guinea pig anti-nephrin (IF, 1:200; BP5030 Acris), rabbit anti-synaptopodin (IF 1:200; Sc-50459 Santa Cruz), mouse anti–β-actin (WB, 1:3000; A2066 Sigma), rabbit anti-laminin (IF, 1:500; L9393 Sigma), Cy5 donkey anti-sheep and Cy5 donkey anti-mouse (IF, 1:200; Jackson ImmunoResearch Laboratories, West Grove, PA), PE-podoplanin (FACS sort, 1:200; clone 8.1.1. BioLegend), AF647-CD73 (FACS sort, 1:2000; clone TY/11.8 BioLegend), and BV421-CD31 (FACS sort, 1:800; clone MEC 13.3 BioLegend).

Animal Experimentation

Animals were housed under defined conditions (22°C, specified pathogen-free, 12-hour day/night cycle) and fed a standard laboratory chow *ad libitum*. They received human care according to the guidelines by the German government. The naive phenotype of male and female mice with podocyte-specific ADAM10 knockout (ADAM10$^{F/F}$ Podo-Cre$^{tg/+}$, hereafter termed "ADAM10Δpod") and control littermate mice (ADAM10$^{F/F}$ Podo-Cre$^{+/+}$, hereafter termed "control") in the C57BL/6 background was analyzed at the age of 10–18 weeks. APN was induced in male and female ADAM10Δpod mice and littermates backcrossed to the C57BL/6 background and aged 13–20 weeks with an APN antibody as previously described.[12] In brief, APN antibody was purified from immunized sheep serum. At the age of 10 weeks, one dose of the antibody (225 μl) was injected intravenously into mice. Preimmune antibody preparation from nonimmunized sheep or naive mice served as the control. After genotype control by PCR and by podocyte immunofluorescence against ADAM10, animals were analyzed at 14 days post-treatment. To isolate glomeruli, mice were euthanized. Kidneys were dissected and perfused with PBS containing magnet beads (4,5 μm; Invitrogen and Spherotec)[21] through the renal arteries. The kidney capsule was removed; the kidney was shredded into small pieces; and then it was digested with 1 mg/ml collagenase (Sigma) and 100 U/ml DNAse (Roche) in HBSS (Thermo Fisher Scientific) for 15 minutes at 37°C under constant agitation, or using the Minilys system (Bertin) to avoid collagenase digestion and cleavage of adhesion molecules (F. Grahammer and T.B.H., University Medical Center Hamburg-Eppendorf [UKE], Hamburg, Germany, unpublished data). The suspension was homogenized through a 100-μm filter and pelleted in a magnetic field. Glomeruli were washed multiple times with HBSS supplemented with 0.05% BSA (Sigma), and preparation quality was controlled microscopically. Part of the intact kidney was prepared for histology.

Mass Spectrometric Analysis of Glomerular Membrane Preparations

Membrane preparations were lysed in STET lysis buffer (1% Triton X-100, 2 mM EDTA, 150 mM sodium chloride, 50 mM Tris pH 7.5) as described before.[22] Lysate was incubated for 20 minutes on ice, with intermediate vortexing, and cleared from cellular debris by a centrifugation step at 16,000 × *g* for 10 minutes at 4°C. A protein amount of 15 μg per sample was subjected to proteolytic digestion with 0.*3* µg LysC (Promega) and 0.15 μg trypsin (Promega), using the filter-assisted sample preparation protocol[23] with 30-kDa Vivacon spin filters (Sartorius). Proteolytic peptides were desalted by stop-and-go extraction with C18 tips.[24] The purified peptides were dried by vacuum centrifugation. Samples were dissolved in 20 μl of 0.1% formic acid. Peptides were analyzed on an Easy nLC 1200 nanoHPLC (Thermo Fisher Scientific), which was coupled online, *via* a Nanospray Flex Ion Source (Thermo Fisher Scientific) equipped with a PRSO-V1 column oven (Sonation), to a Q-Exactive HF mass spectrometer (Thermo Fisher Scientific). An amount of 1.3 μg of peptides was separated on an in-house-packed C18 column (30 cm×75 μm ID, ReproSil-Pur 120 C18-AQ, 1.9 μm; Dr. Maisch GmbH) using a binary gradient of water and acetonitrile supplemented with 0.1% formic acid (0 minute, 2% acetonitrile; 3:30 minutes, 5% acetonitrile; 137:30 minutes, 25% acetonitrile; 168:30 minutes, 35% acetonitrile; 182:30 minutes, 60% acetonitrile) at a column temperature of 50°C and a flow rate of 250 nl/min. A data-dependent acquisition method was used. Full mass-spectrometry (MS) scans were acquired at a resolution of 120,000 (m/z range, 300–1400; AGC target, 3E+6). The ten most intense peptide ions per full MS scan were selected for peptide fragmentation (resolution, 15,000; isolation width, 2.0 m/z; AGC target, 1E+5; NCE, 26%). A dynamic exclusion of 120 seconds was used for peptide fragmentation. The data were analyzed with Maxquant version 1.6.1.0 software (maxquant.org; Max Planck Institute, Munich, Germany).[25] The MS data were searched against a reviewed, canonic FASTA database of *Mus musculus* from UniProt (downloaded January 17, 2018; 16,954 entries). Trypsin was defined as protease. Two missed cleavages were allowed for the database search. The first-search option was used to recalibrate the peptide masses within a window of 20 ppm. For the main search peptide and peptide fragment, mass tolerances were set to 4.5 and 20 ppm, respectively. Carbamidomethylation of cysteine was defined as static modification. Acetylation of the protein amino-terminus and oxidation of methionine was set as variable modifications. The false discovery rate for both peptides and proteins was adjusted to <1%. Label-free quantification of proteins required at least two ratio counts of razor peptides. Only unique peptides were used for quantification.

MS Analysis of Glomerular Cell Types

Glomerular cells were separated using a newly developed timMEP method.[26] (preprint) Briefly, glomeruli were dissolved in digestion buffer containing 1000 μg/ml Liberase TL (Roche), 100 U/ml DNase1 (Roche), 10% FCS, 1% ITS, 1% penicillin/streptomycin, 25 mM *N*-2-hydroxyethylpiperazine-*N*'-2-ethanesulfonic acid (HEPES) dissolved in 1× RPMI Medium 1640 (Gibco). Glomeruli were incubated for 2 hours at 37°C, centrifuged at 1400 rpm, and repeatedly and diversely mechanically stressed. A DynaMag was used to separate glomerular remnants and DynaBeads from singular cells. After 5 minutes in the DynaMag, the single cell–containing supernatant was collected. Cells were pelleted (10 minutes, 4°C, 1000 × *g*) and washed once with

MACS buffer (PBS with 0.5% BSA and 2 mM EDTA). Subsequently, cells were stained for 30 minutes with the cell-specific antibodies podoplanin (podocytes), CD73 (mesangial cells), CD31 (endothelial cells), and a live/dead stain (near-IR fluorescent reactive dye, 1:4000; Invitrogen), and then FACS sorted. Proteins were identified by MS as described.[26] (preprint) Differentially expressed proteins were defined by ANOVA with a false discovery rate–corrected *P* value of <0.01 to adjust for multiple testing.

Microarray Analysis of Human Biopsy Specimens

Human kidney biopsy specimens and Affymetrix microarray expression data were obtained within the framework of the European Renal cDNA Bank – Kröner-Fresenius Biopsy Bank (ERCB-KFB).[27] Biopsy specimens were obtained from patients after informed consent and with approval of the local ethics committees. Biopsy specimens were processed as previously reported.[28] Published gene expression profiles (Affymetrix GeneChip Human Genome U133A and U133 Plus2.0 Arrays; GSE 99340, GSE32591, GSE35489, and GSE37463) used in this study came from patients with different CKDs (diabetic nephropathy [DN], minimal change disease [MCD], hypertensive nephropathy, IgA nephropathy, FSGS, membranous nephropathy [MN], lupus nephritis, and ANCA-associated GN). Pretransplantation kidney biopsy specimens from living donors (*n*=42) were used as control renal tissue. CEL file normalization was performed with the Robust Multichip Average method using RMAExpress (version 1.0.5) and the human Entrez Gene custom CDF annotation from BrainArray version 18 (http://brainarray.mbni.med.umich.edu/Brainarray/default.asp). The log-transformed dataset was corrected for batch effects using ComBat from the GenePattern pipeline (http://www.broadinstitute.org/cancer/software/genepattern/). To identify differentially expressed genes the SAM (Significance analysis of Microarrays) method was applied using TiGR (MeV, version 4.8.1).[29]

Determination of Urine and Serum Parameters

Urine samples were collected over 3–5 hours in a metabolic cage with free access to water. Urine albumin content was quantified using a commercially available ELISA system (Bethyl), according to the manufacturer's instructions, using an ELISA plate reader (BioTek), as described.[13] Values were standardized against urine creatinine values of the same individuals, determined according to Jaffe, and plotted. Serum BUN values were determined by automatic measurement by Laboklin (Schweinfurt, Germany).

Murine Podocyte Cell Culture and Cell-Based APN Model Experimentation

Undifferentiated murine podocytes[30] were cultured in RPMI supplied with 10% FCS, 1% penicillin/streptomycin, 15 mM HEPES, 1 mM sodium pyruvate, and 10 U/ml IFNγ at 32°C and 5% carbon dioxide. For differentiation, IFNγ was removed from the medium and podocytes were cultured at 37°C and 5% carbon dioxide for at least 14 days. To analyze podocytes in the APN model, cells were treated for 24 hours with the indicated antibody concentrations in standard medium, and then prepared for further analysis. Preimmune antibody treatment served as the

control. Dependency on ADAM10 activity was tested by application of 2 μM of the ADAM10 inhibitor GI254023X (Iris Biotech) to a control sample. Treatment with 5 μM ionomycin (Sigma) 30 minutes before cell harvest or staining served as the positive control for stimulated activity of ADAM10. When indicated, cells were additionally treated with 1 μM of the γ-secretase inhibitor DAPT to illustrate changes in ADAM10-generated, C-terminal fragments (CTFs).

Adhesion Assay

Differentiated murine podocytes were detached from the culture dish by trypsin/EDTA and regeneration of surface molecules was allowed for 30 minutes at 37°C, under constant agitation. Cells were seeded in a 96-well plate and incubated with preimmune or APN antibody and DMSO or the ADAM10 inhibitor GI254023X, as indicated, for 24 hours. Control samples were incubated for 1 hour with 5 μM ionomycin. Medium was removed and cells were stained with crystal violet solution (0.5% wt/vol crystal violet in 20% vol/vol methanol) for 5 minutes at room temperature. Nonadherent podocytes were depleted by multiple PBS washing steps. Overnight, adherent podocytes were lysed in the plate in isopropanol at room temperature. Cell adherence was quantified by determining lysate extinction at 562 nm (six replicates per condition).

Immunofluorescence Imaging

Kidney samples were either embedded in Tissue-Tek O.C.T. compound (Sysmex) or in paraffin. Cryosections (5 μm thick) were air dried and fixed in 4% paraformaldehyde/PBS. Human biopsy samples were provided by the department of nephropathology at the UKE. Paraffin sections were cut to a thickness of 3 μm, deparaffinized, and rehydrated to water. Antigen retrieval was performed using proteinase K (1:2000; Sigma) or heat retrieval in pH9 or pH6 buffer (Dako). After multiple PBS washing steps, slices were permeabilized in 50 mM ammonium chloride. Samples were blocked in 5% normalized horse serum (Vector) and 0.05% Triton X-100 in PBS and incubated with primary antibodies in blocking solution at 4°C overnight. After multiple washing steps with PBS, secondary antibody was added in blocking solution for 30 minutes at room temperature (all 1:200; Jackson ImmunoResearch Laboratories). Nuclei were counterstained for 5 minutes with draq5 or Hoechst (1:1000; both Molecular Probes). For immunofluorescence of cultured podocytes, cells were seeded on coverslips and treated as indicated. Cells were washed with PBS and fixed in 4% paraformaldehyde in PBS for 20 minutes at room temperature. Permeabilization was carried out in 0.2% saponin in PBS for 5 minutes, and then stopped with 0.12% glycine, 0.2% saponin, and PBS for 10 minutes. Samples were blocked for 2 hours in 10% FCS, 0.2% saponin, and PBS and incubated with primary antibodies overnight at 4°C in a wet chamber. After several washing steps with 0.2% saponin in PBS, secondary antibody was added in blocking buffer for 1 hour at room temperature. Nuclei were counterstained with 4′,6-diamidino-2-phenylindole (Sigma). Stainings were analyzed using a LSM510 Meta, a LSM800 with Airyscan (both Zeiss), or an Olympus F1000 using the LSM software, ZENBlue software (all Zeiss), or Fluoview software (Olympus).

EM Imaging

For transmission EM, samples were fixed in 6% glutaraldehyde in 0.1 M phosphate buffer, post-fixed in 2% osmium tetroxide and embedded in Araldite. Ultrathin sections were stained with uranyl acetate and lead citrate, and then analyzed using an EM900 Zeiss electron microscope.

SDS–Freeze-Fracture Replica Labeling with Immunogold

Immunogold labeling of replicas was performed as previously described.[31] Briefly, C57BL/6 wild-type kidneys were quickly removed and incubated overnight at 4°C in a fixative containing 2% paraformaldehyde and 15% saturated picric acid in 0.1 M phosphate buffer. Sections (100 μm thick) were cut and cryoprotected overnight in phosphate buffer with 30% glycerol, and then frozen using a high-pressure freezing machine (HPM100; Leica). Frozen samples were freeze fractured at −140°C and coated by deposition of carbon (5 nm thickness), platinum (2 nm), and carbon (18 nm) in a freeze-fracture replica device (BAF 060; BAL-TEC). Replicas were digested for 24 hours at 80°C in a solution containing 2.5% SDS and 20% sucrose in 15 mM Tris buffer at pH 8.3. Replicas were washed in 50 mM Tris-buffered saline (TBS) containing 0.05% BSA (Roth) and 0.1% Tween 20 (Roth), and then incubated in a blocking solution (5% BSA). Subsequently, replicas were incubated in primary antibody against ADAM10 (1:25) prepared in 50 mM TBS containing 1% BSA and 0.1% Tween 20 overnight at room temperature. Replicas were subsequently rinsed in TBS, blocked, and incubated with a secondary gold-coupled 12 nm antibody (anti-rat IgG, 1:30; Jackson ImmunoResearch Laboratories) diluted in TBS containing 1% BSA overnight at 15°C. Replicas were subsequently rinsed in TBS and ultrapure water and mounted on 100-mesh grids. The labeled replicas were examined using a transmission electron microscope (CM100; Philips).

Quantitative RT-PCR Analysis

Total mRNA was extracted from isolated glomeruli, using phenol/chloroform, or from cultured podocytes, according to the NucleoSpin RNA Plus Kit (Macherey-Nagel) protocol. Glomeruli were lysed with Tungsten Carbide Beads (Qiagen) and TRIzol (Ambion) in a TissueLyser II (Qiagen) at 30 Hz for 1 minute. RNA was separated using 1/6 volume chloroform. RNA was precipitated using isopropanol at 4°C for 30 minutes, and the RNA pellet was washed three times with 80% ethanol. RNA was dissolved in purified water and 200 ng of RNA was reverse transcribed with a random hexamer primer (Invitrogen) and MMLV reverse transcription (NEB). mRNA expression was quantified with a QuantStudio 3 (Applied Biosystems) AbiPrism NN8860 using SYBR green as recently described.[32] The exon-spanning primer pairs to murine cDNA we used are listed in Supplemental Table 1. 18S was used as an internal control to correct for small variations in RNA quality and cDNA synthesis, as described by AbiPrism. Amplicons of random samples for each primer pair were determined by automatic PCR sequencing to demonstrate the specificity of the PCR reaction (data not shown). Glomerular relative gene expression was calculated using the $\Delta\Delta$CT method. To quantify cDNA levels of cultured podocytes, a quantitative RT-PCR (qRT-PCR) with technical duplicates was run on the basis of the Universal ProbeLibrary system (Roche). CT values were calculated, normalized to a housekeeper gene, and presented as multiples of the control.

Cell-Surface Protein Biotinylation

After treatment as depicted, differentiated murine podocytes were washed with PBS-CM (0.1 mM calcium chloride/1mM magnesium chloride in PBS). Subsequent biotinylation was performed with 1 mg/ml Biotin (#21331; Thermo Fisher Scientific) in PBS-CM for 30 minutes at 4°C, and then stopped in quenching buffer (50 mM Tris in PBS-CM, pH 8.0) for 10 minutes at 4°C. Cells were washed several times and transferred to a tube for lysis. Cells were resuspended in lysis buffer (50 mM Tris, 150 mM sodium chloride, 0.1% SDS, 1% Triton X-100, 2× protease inhibitor, pH 7.4) and sonicated. After incubation at 4°C for 30 minutes, cells were sonicated again and supernatant was separated by centrifugation. Equal protein amounts were attributed to streptavidin agarose (#20359; Thermo Fisher Scientific) precipitation of biotinylated proteins (1 hour, 4°C, constant inverting). Beads were washed several times in lysis buffer and the supernatant was analyzed *via* immunoblot. Equal amounts of lysate before precipitation served as the input control.

Sample Lysis and Immunoblot Analysis

For immunoblot analysis, podocyte cell samples were lysed in 1 mM EGTA, 250 mM saccharose, 1% vol/vol Triton X-100, 2× concentrated protease inhibitor in 5 mM Tris–hydrogen chloride, pH 7.4. Nonsoluble components were pelleted, and supernatant was separated with SDS–gel electrophoresis and transferred to a nitrocellulose membrane to perform immunoblotting. Membranes were blocked with 5% dry milk powder in TBS/Tween 20 (TBS/T) and incubated with primary antibodies in 5% BSA in TBS/T overnight. Membranes were washed in TBS/T and incubated with secondary antibodies diluted 1:10.000–1:15:000 in 5% BSA in TBS/T. After additional washing steps, chemiluminescence detection was performed with an ImageQuant LAS 4000 camera. Isolated glomeruli were lysed in T-Per (Thermo Fisher Scientific) containing 1 mM sodium fluoride, 1 mM sodium vanadate, 1 mM calyculin A, and cOmplete Protease Inhibitor (Roche), and denatured in SDS solubilization buffer. Samples were separated on a 4–12% Mini Protean TGX gel (Bio-Rad) in a Tris-glycine migration buffer (0.25 M Tris, 1.92 M glycine, 1% SDS, pH 8.3). Protein transfer was performed in transfer buffer (0.192 M glycine, 25 mM Tris base, 20% ethanol in water) in a TransBlot Turbo System (Bio-Rad). After the transfer, all proteins were visualized by ponceau staining. Polyvinylidene difluoride membranes (Millipore) were blocked (5% nonfat milk) before incubation with primary antibodies diluted in Superblock blocking reagent (Thermo Fisher Scientific) or nonfat milk. Binding was detected by incubation with horseradish peroxidase–coupled secondary antibodies (1:10,000; 5% nonfat milk). Protein expression was visualized with ECL SuperSignal (Thermo Fisher Scientific), according to the manufacturer's instructions, on an Amersham Imager 600 (GE Healthcare). Immunoblots were analyzed using software from ImageJ.[33] Ponceau and *β*-actin stainings of the same membrane are shown and were used as loading control and for densitometric normalization. Bands of the same membrane are shown, fine dashed white lines indicate where bands were not adjacent to another on the membrane.

Statistical Analyses

Cell culture data were depicted as mean±standard deviation if not indicated otherwise. A *t* test was applied to compare groups. If data were not normally distributed or variances were unequal, a Mann–Whitney *U* test was performed. Mouse data were given as mean±SEM. The means were compared using the Mann–Whitney *U* test to enable robust conclusions on effect significance in cases of departure from normality associated with small sample sizes. For comparison of more than two groups, the one-way ANOVA was used with the Tukey multiple comparison test. Significance was set at $P<0.05$. The replicates used were biologic replicates, which were measured using different samples derived from distinct mice. All animals were littermates and were blindly assigned to the experimental groups.

Results

Podocytes Specifically Express ADAM10

Proteomic analyses from glomerular membrane preparations identified the expression of ADAM10, ADAM15, ADAM17, ADAM22, ADAM9; ADAMTS1, ADAMTS5, and ADAMTSL4. Glomerular cell resolution was increased by performing proteomic analyses from FACS-sorted podocytes and mesangial and endothelial cells.[26 (preprint)] Molecular protein expression levels indicated murine podocytes mainly express ADAM10, whereas the close ADAM10 homolog, ADAM17, is mainly expressed by glomerular endothelial and mesangial cells (Figure 1A). Proteomic analyses further identified proteins relevant to the regulation of ADAM10 activity in both databases (Supplemental Table 2). All three glomerular cell types expressed the AP2 subunits and SAP97/Dlg1, which are relevant for ADAM10 trafficking and recycling. Endothelial cells expressed Tetraspanin 14 (Tspan14), whereas Tspan15 and Tspan5 were abundant in podocytes, suggesting a glomerular cell–type specific regulation of ADAM10 activity and/or substrate specificity. Therefore, we focused on the analysis of the putative role of ADAM10 for podocyte function. First, podocyte ADAM10 expression was validated and subcellularly localized. ADAM10 localized in close proximity to the GBM protein laminin, toward the podocyte FP plane of the GFB (Supplemental Figure 1A). Localization studies of ADAM10 relative to the SD bridging protein nephrin demonstrated a partial colocalization of both proteins (Figure 1B, Supplemental Figure 1B). Freeze-fracture Immunogold EM studies confirmed the predominant FP localization of ADAM10 in mouse glomeruli (Figure 1C).

Generation of ADAM10-Deficient Podocytes

Mice deficient for ADAM10 ($ADAM10^{F/F}$, NPHS2 [Podocin]-$Cre^{tg/+}$) were generated by breeding homozygous floxed $ADAM10^{F/F}$ mice[34] to NPHS2-Cre transgenic mice (Figure 2A).[35] Successful ADAM10 deletion was seen by PCR detecting both the exon2-deleted (*Δ*ADAM10, 700 bp) and the floxed ADAM10 (ADAM10 flox, 2000 bp) allele in glomerular samples (Figure 2B).[36] Reduced glomerular ADAM10 protein levels were seen by immunoblot (Figure 2C). Although the immature ADAM10 proform was barely detectable, mature ADAM10 was strongly reduced in Cre transgenic mice. The weak, residual ADAM10 levels noted in ADAM10-deficient glomeruli could be attributed to a tubular contamination of the glomerular preparations. Immunofluorescence

exhibited a complete loss of podocyte ADAM10 expression (Figure 2D) in Cre transgenic mice, demonstrating the successful generation of podocyte-specific, ADAM10-deficient (ADAM10Δpod) mice.

ADAM10 Is Dispensable for Normal Podocyte Development

ADAM10 proteolysis is the initiating event in Notch signaling, an important regulator of embryonal development in glomerular endothelial cells,[37] among others.[16,38] During podocyte development, Notch signaling was depicted to be essential, whereas it is silenced in the adult.[39,40] Because the NPHS2 promoter is active from the capillary-loop stage onward,[35] we assessed for podocyte developmental defects in ADAM10Δpod mice. No glomerular or tubulointerstitial alterations were detected by light-microscopy evaluation (Figure 3A). Podocyte integrity was maintained in ADAM10Δpod mice, as depicted by the preserved localization of the podocyte cytoskeleton-associated synaptopodin (Supplemental Figure 2) and by the tightly meandering nephrin pattern at the SD in ADAM10Δpod mice (Figure 3B). EM confirmed the normal morphology of ADAM10-deficient podocytes (Figure 3C). Functionality of the ADAM10Δpod GFB was monitored by urinary albumin-creatinine measurements (Figure 3D), and was within the normal range.[12] Taken together, our data demonstrate the successful generation of mice with a podocyte-specific ADAM10 deficiency, in which glomerular/podocyte development was unaffected.

Glomerular ADAM10 Expression Is Altered in Nephrotic Syndrome

Podocyte injury typically results in a restructuring of FPs by actin-cytoskeletal rearrangement and by alteration of the podocyte-GBM and podocyte-podocyte interaction/adhesion.[41] Because ectodomain shedding of cell-cell or cell-GBM proteins could be pathophysiologically relevant in this setting, we evaluated to what extent ADAM10 was regulated, on a transcriptional level, in human glomerular diseases (Figure 4A). We detected a glomerular upregulation of *ADAM10* in DN; hypertensive nephropathy; IgA nephritis; systemic lupus erythematosus; rapid progressive GN; and, to a lesser extent, in MCD, FSGS, and MN. Analyses of glomerular ADAM10 localization in these disease conditions (Figure 4B, Supplemental Figure 3) demonstrated that, in contrast to mice, ADAM10 expression was barely detectable in healthy human glomeruli. In MCD, no obvious podocyte ADAM10 expression was seen. In MN, an autoimmune disease in which podocyte injury is mediated by autoantibodies to PLA_2R1[42] or THSD7A,[43,44] we could observe a podocyte induction of ADAM10, which was precisely localized in podocyte structures above the disrupted nephrin pattern, most likely representing primary podocyte processes. In FSGS, the ADAM10 signal was only faintly observed at the GFB in two layers, one colocalizing with nephrin (therefore, at the FP plane) and one located toward the endothelial lining (most likely representing endothelial ADAM10).

Because we observed a varying pattern of glomerular ADAM10 expression in human podocytopathies, we analyzed ADAM10 expression in murine APN (Figure 4C, Supplemental Figure 4). APN is induced by injection of polyclonal sheep antibodies directed to podocyte antigens, which results in an immune-complex GN with subepithelial immune deposits, FPE, nephrotic syn-

drome, and (in severe injury forms) in endothelial swelling.[12,13] ADAM10 expression was markedly enhanced in injured podocytes in APN. Interestingly, we observed an additional induction of ADAM10 in glomerular endothelial cells of APN-treated mice, which was absent in ADAM10Δpod APN mice (Figure 4C), suggesting a podocyte-specific, ADAM10-dependent response in glomerular endothelial cells. Immunoblot analyses further confirmed an APN-induced upregulation of ADAM10 in glomeruli (Figure 4D). Together, these human and murine data argue for ADAM10 as a potentially important regulator of podocyte injury, which can be functionally investigated in the APN model.

ADAM10 Deficiency Rescues Podocyte Damage in the APN Model

APN was induced in ADAM10Δpod and control littermates (Figure 5A), and disease severity was compared on day 14. Renal function was ameliorated in ADAM10Δpod compared with control littermates when assessing BUN levels (Figure 5B). Although control littermates developed nephrotic-range proteinuria, ADAM10Δpod APN mice exhibited a significantly decreased urinary albumin loss (Figure 5C). Due to the strong variability in proteinuria, light-microscopy evaluation was performed in animals with comparable proteinuria. The glomerular structure was mostly preserved in ADAM10Δpod in comparison with control APN littermates, despite similar tubulointerstitial injury in both genotypes, characterized by dilated tubuli filled with proteinaceous casts (Figure 5D, Supplemental Figure 5). To rule out a differential induction of APN between the genotypes, we controlled for the glomerular deposition of the injected sheep IgG (Figure 5E) and for the intrinsic reaction of mice to the foreign sheep IgG.[12,13] Both, the deposition of sheep IgG and the deposition of mouse IgG (Supplemental Figure 6) at the GFB was comparable in linearity and intensity between ADAM10Δpod and control littermates. Specific analyses of podocyte integrity demonstrated a severe disruption of synaptopodin and nephrin localization in control APN littermates, which was ameliorated in ADAM10Δpod mice. Besides loss of linearity, nephrin was internalized (Supplemental Figure 7), a typical hallmark of podocyte injury.[45,46] High-resolution microscopy of nephrin exhibited marked FPE in control APN littermates, whereas ADAM10Δpod mice only exhibited focal areas of FPE (Figure 5F, Supplemental Figure 8A). This high-resolution, confocal finding was validated by transmission EM (Figure 5G), where APN antibody–treated control animals showed significant FPE, whereas ADAM10Δpod animals showed broadened FPs after APN-antibody application. Even those FPs overlying electron-dense deposits were preserved (Supplemental Figure 8B). Taken together, these observations indicate ADAM10 deficiency is sufficient to protect animals from APN antibody–induced structural and functional disturbances.

APN-Induced Detachment of Podocytes Is Mediated by ADAM10, Independent of Notch Signaling

ADAM10 activity in the APN model could favor podocyte Notch signaling and/or cleavage of cadherin cell-adhesion proteins and thereby Wnt/β-catenin signaling, resulting in podocyte loss and nephrotic syndrome. First, we quantified podocyte loss in the setting of APN between genotypes (Figure 6A). Podocyte number per glomerular tuft area was not different between untreated

ADAM10Δpod and control littermates. In APN, control littermates exhibited a significant podocyte loss, which was less prominent in ADAM10Δpod mice.

The underlying molecular effects of ADAM10 on podocytes were first investigated in cultured murine podocytes.[30] To verify that a cell-based approach is suitable to analyze ADAM10 function, APN antibodies were applied to cultured podocytes. APN-treated podocytes revealed ADAM10-dependent morphologic alterations (Supplemental Figure 9). Further, podocyte adhesion was significantly reduced upon APN-antibody treatment, which was rescued to an intermediate level upon additional incubation with the ADAM10 inhibitor GI254023X[47] (Figure 6B). In line with a role of ADAM10 in cell detachment, stimulation of ADAM10 activity with ionomycin[48,49] also significantly reduced podocyte cell adhesion.

Because podocyte detachment was dependent on ADAM10 activity, we studied proteolytic shedding of ADAM10 substrates that can potentially affect podocyte morphology or adhesion. First, ADAM10-mediated Notch signaling was addressed by qRT-PCR analysis of Notch and of Notch-downstream genes of the Hes and Hey family. We observed an activation of Notch signaling in cultured podocytes and *in vivo* after exposure to APN antibodies; however, this was not ADAM10 dependent, as revealed by the addition of GI254023X in culture (Supplemental Figure 10A) or by the failure to attenuate the APN antibody–induced glomerular expression of Notch and Notch-downstream genes *in vivo* by podocyte ADAM10 deficiency (Supplemental Figure 10B). In conclusion, we could not confirm a role for ADAM10 in activating podocyte Notch signaling in APN.

ADAM10-Mediated Cadherin Cleavage Weakens Cell-Cell Interactions

Because podocyte adhesion was impaired upon APN-antibody treatment in culture and *in vivo* in an ADAM10-dependent manner, we determined the effect of ADAM10 on shedding of podocyte-expressed adhesion molecules. We first searched for the downstream activation of the Wnt/*β*-catenin signaling pathway by qRT-PCR in culture and *in vivo*, because Wnt signaling is a known stimulus of podocyte injury[20] and is activated upon ADAM10-dependent cadherin adhesion molecule cleavage.[50,51] In cultured podocytes (Supplemental Figure 11), the classic Wnt response genes cyclin D1 (*Ccnd1*) and *β*-enolase (*Eno3*) were weakly induced upon APN-antibody stimulation. This induction could be rescued by GI254023X treatment, suggesting these two genes are induced in response of APN antibody–induced ADAM10 activity, whereas others were not (Supplemental Figure 11).

Consistent with the notion that the podocyte SD is a modified adherens junction,[2] two cadherins have been described to associate with ZO-1 and with the catenins of the SD, namely P-cadherin (CDH3) and the protocadherin FAT1.[2,52,53] P-cadherin is a known target of ADAM10.[54] N-cadherin (CDH2), albeit representing a central target to ADAM10 in neurons and fibroblasts,[14] has not yet been localized to human or murine podocytes *in vivo*. Changes in cell-surface expression of P-cadherin, E-cadherin, and FAT1 could not be monitored in cultured podocytes due to technical issues. However, membrane biotinylation of podocytes exposed to APN antibody revealed decreased full-length (FL) N-cadherin cell-surface levels, which could be rescued by GI254023X (Figure 6C). The analysis of cell lysates did not point toward a change in total N-cadherin levels,

excluding the contribution of transcriptional effects to the reduction of surface levels by APN-antibody treatment. N-cadherin shedding by ADAM10 yields a membrane-bound CTF that is further proteolyzed by the γ-secretase complex. To demonstrate ADAM10-mediated N-cadherin CTF generation in podocytes, N-cadherin proteolysis was analyzed in the presence of the γ-secretase complex inhibitor DAPT (Figure 6D). Exposure to APN antibodies increased the generation of the N-cadherin CTF over time (16 hours and 24 hours), which was accompanied by a decrease in FL N-cadherin, which supports the argument for ongoing ectodomain shedding in podocyte injury. GI254023X suppressed both the generation of N-cadherin CTF and the decline of N-cadherin FL. Immunofluorescence staining of N-cadherin in cultured podocytes confirmed the ADAM10-dependent cell-surface reduction observed in the biotinylation experiment (Supplemental Figure 12). Together, these data argue for N-cadherin to be a relevant podocyte ADAM10 substrate in culture.

To convert our cell-based observations to the *in vivo* situation, we analyzed the effect of podocyte-specific ADAM10 deficiency on cell-cell adhesion molecule expression and distribution. To this end, no robust data could be obtained for FAT1. We could, however, validate the colocalization of P-cadherin and N-cadherin with nephrin on the apical side in podocyte precursors at the capillary phase of developing murine glomeruli (Supplemental Figure 13). In mature naive glomeruli, no P-cadherin (Supplemental Figure 14A) and only faint intraglomerular N-cadherin (Supplemental Figure 15A) abundance could be observed. N-cadherin was localized inside podocytes and in primary podocyte processes. No difference in basal N-cadherin or P-cadherin levels was observed between naive ADAM10Δpod and control littermates (Supplemental Figures 14B and 15B). Together, these findings suggest that, in developing podocytes, the adherens junction contains a larger spectrum of cell-cell adhesion molecules, besides nephrin, than in the mature modified adherens junction (the SD).

In the course of injury, podocytes dedifferentiate and reactivate embryonal gene expression patterns. One consequence of this is that production of typical proteins of healthy podocytes, such as nephrin, is reduced. We hypothesized that nephrin loss in podocyte injury could potentially be counterbalanced by re-expression of embryo-expressed P-cadherin and N-cadherin as a "rescue" mechanism. In line with this idea, N-cadherin represents the main cell-cell adhesion protein at the SD in birds because they physiologically lack nephrin,[55] demonstrating that N-cadherin can be expressed in podocytes, especially in the absence of nephrin. Therefore, we analyzed whether, in APN, the abundance of N-cadherin and P-cadherin was enhanced in ADAM10-deficient podocytes, where the cleavage of these cell-cell adhesion proteins should be absent or strongly reduced. In APN, glomerular lysates of ADAM10Δpod mice exhibited higher levels of N-cadherin (Figure 7A) compared with control littermates, which was not related to differences in podocyte count, because α-actinin 4 levels were comparable. ADAM10Δpod APN mice exhibited an enhanced podocyte immunosignal for N-cadherin (Figure 7B) and P-cadherin (Figure 7C) in comparison with proteinuria-matched control littermates. P-cadherin localized to the podocyte rather than the endothelial aspect of the GFB, and N-cadherin localized to podocyte primary processes. Analyses of N-cadherin localization in patients with autoantibody-mediated glomerular injury, such as MN and anti-GBM GN, exhibited basal N-cadherin localization in the podocyte cytoplasm and primary processes, which was comparable to the localization observed in mice. Interestingly, an additional N-cadherin localization at the plane of nephrin was observed in both

MN and anti-GBM GN, especially in areas where nephrin was absent (Figure 7D).

Whereas the ectodomain of cadherins confers specific adhesive binding, the cytoplasmic domain mediates the structural and signaling activities required for adhesion through its interaction with *β*-catenin.[56] Cadherin levels influence *β*-catenin levels[57] and thereby set threshold for Wnt signals. N-cadherin cleavage promotes *β*-catenin activation and cytoplasmic and nuclear localization.[58] We assessed the glomerular levels and localization of total *β*-catenin to further strengthen the finding of reduced N- and P-cadherin cleavage in ADAM10*Δ*pod APN mice. Glomerular *β*-catenin levels were lower in ADAM10*Δ*pod APN mice in comparison with control littermates (Figure 8A). Control APN littermates exhibited an enhanced immunosignal for *β*-catenin in the cytoplasm of glomerular endothelial cells and podocytes. Further, podocytes showed nuclear *β*-catenin staining, which was absent in ADAM10*Δ*pod APN mice (Figure 8B, Supplemental Figure 16). Similarly to the observations in cultured podocytes (Supplemental Figure 11), glomerular qRT-PCR analyses of Wnt response genes exhibited an ADAM10-dependent expression of *Axin2*, *Ccnd1*, and *Fn1* in APN mice (Figure 8C), supporting an ADAM10-dependent activation of the Wnt/*β*-catenin pathway in the nephritis model. Other Wnt response genes such as *Eno3* and *Tiam1* exhibited no enhanced expression upon APN induction.

Taken together, these data suggest ADAM10-mediated cleavage of injury-induced cell-cell adhesion molecules at podocytes is pathogenetically associated with podocyte loss and nephrotic syndrome through enhanced activation of the Wnt/*β*-catenin signaling pathway (summarized in Figure 8D).

Discussion

The pathophysiologic factors driving podocyte injury and loss range from cytoskeletal reorganization, reactivation of embryonic programs, and alteration of podocyte adhesion to the GBM. In this study, we asked whether there was a role for ectodomain cleavage of transmembrane molecules by ADAM10 in podocyte biology.

Contrary to recent findings that ADAM10-dependent Notch signaling is required for the proper development of the glomerular endothelium,[37] ADAM10-dependent Notch signaling for podocyte development does not seem to be of major importance. This could be related to the expression of Tspan15 by podocytes. Tspan15 inhibits ADAM10-mediated Notch activation upon ligand binding,[59] potentially explaining the lack of morphologic and functional podocyte defects in naive ADAM10*Δ*pod mice. Interestingly, although mice exhibited a prominent podocyte ADAM10 expression, this was not observed in human glomeruli, contradicting reports by Gutwein *et al.*,[60,61] where ADAM10 was shown in cultured human podocytes and in healthy human biopsy specimens. We were not able to overcome this discrepancy, despite using four different ADAM10 antibodies, which all showed a strong tubular apical membrane but no convincing podocyte ADAM10 expression in kidney sections.

Podocyte-expressed proteins described to be shed by ADAM10 are the L1 adhesion molecule[60] and the chemokine CXCL16, which is involved in the uptake of oxidized LDL.[62] We found that

ADAM10 is localized at murine FPs. Therefore, we proceeded to assess the abundance of known ADAM10 cell-cell adhesion substrates in ADAM10Δpod mice, because these could represent new podocyte targets of ADAM10. Cell-cell adhesion proteins found at the SD[63–65] are the podocyte-specific protein nephrin, and the nonpodocyte-restricted proteins FAT1 and P-cadherin, the latter representing a known ADAM10 substrate. We could not observe changes in nephrin or P-cadherin levels in podocytes of naive ADAM10Δpod mice. Therefore, we extended our search and identified a low abundance of N-cadherin in podocytes and glomerular endothelial cells of naive mice, which (like P-cadherin) did not differ between ADAM10Δpod and control littermates. Nonetheless, this is (to the best of our knowledge) the first report of a podocyte N-cadherin expression in mice. Our analyses further demonstrated prominent P- and N-cadherin colocalization with nephrin in developing glomeruli from the capillary-loop stage onward, suggesting the developing SD contains a larger arsenal of cell-cell adhesion proteins than the mature SD, and the abundance of cadherins is reduced upon maturation. Of note, the mature SD in birds does not contain nephrin as a cell-cell adhesion protein but N-cadherin instead,[55] demonstrating cadherins can functionally compensate for nephrin—a process potentially interesting in podocyte injury, where nephrin is removed from the SD by endocytosis.[66] In terms of an injury-related reactivation of an embryonal SD program, the expression of cadherins, such as N-cadherin, might potentially compensate for nephrin internalization/loss in the setting of GN. Of note, Tspan15, which is preferentially expressed in podocytes, mediates ADAM10-dependent shedding of N-cadherin by fostering its transport to the cell surface,[59] suggesting a role for the Tspan15-ADAM10–N-cadherin axis in podocyte injury.

We established that ADAM10 activity is essential for the progression of podocyte injury and loss in the setting of experimental GN. After antibody-mediated podocyte injury, ADAM10 directly affected cell adhesion by shedding of N-cadherin in a cell-based approach and *in vivo*. A role for ADAM10 in podocyte injury has been proposed previously, because ADAM10 is found in urinary vesicles derived from patients with GN.[60] Due to the strong expression of ADAM10 at the apical membrane of the renal tubular system, the ADAM10 present in urinary vesicles could, however, be derived from both the podocyte and the tubular compartment. Nonetheless, in agreement with the assumption that ADAM10 could be involved in the development of podocyte injury, we demonstrated an induction of ADAM10 transcript in a variety of human GN and of ADAM10 protein in human antibody-mediated injury, such as MN and anti-GBM GN. In line with this, APN mice demonstrated an increase in glomerular ADAM10, which was, however, not restricted to podocytes but also present on the endothelium. The abundance of ADAM10 on podocytes has been suggested to decrease in DN[62] and in human MN,[61] which is in contrast to our transcriptional and histologic findings that might originate from technical differences or from differences in the patient cohorts (unclassified MN by Gutwein *et al.* [61] and PLA_2R1-positive MN in our study).

ADAM10 mediates the proteolysis of important surface proteins—such as adhesion proteins, cytokines, and the Notch receptor—in a cell type–dependent manner.[14,15,67,68] The consequences of such shedding events can be diverse in different tissues and have been partially revealed by the analysis of conditional and tissue-specific ADAM10-depleted mice.[34,36,69–71] Further, through the initial shedding events, ADAM10 modulates the activity of downstream signaling pathways, which is illustrated by Wnt and Notch hyperactivation.[19,20,72] Studies suggest Notch signaling

drives nephritis, revealing the potential of ADAM10 inhibition in this context. In our study, ADAM10 deficiency attenuated the disruption of the SD, a finding not related to an ADAM10-dependent activation of podocyte Notch shedding. Of note, some of the analyzed transcripts are not solely regulated by Notch but also by TGF*β* signaling (as for *Hey1*).[73] Finally, Notch expression itself is known to be regulated by a positive feedback loop. However, upregulation of *Notch1* in culture and *in vivo* after APN antibody exposure was not dependent on ADAM10 activity, because it could not be suppressed by GI254023X and was persistent in ADAM10*Δ*pod mice. *Notch2* did not reveal significant effects. These observations are in line with ADAM10 being dispensable for podocyte development, arguing for a different protease responsible (or compensating) for initiation of Notch signaling in podocytes.

During the establishment of nephritis, ectodomain shedding of cadherins by ADAM10 may directly contribute to podocyte alterations. This is supported by our observation that N-cadherin shedding was induced, and podocyte adhesion was reduced, after APN-antibody application in cultured podocytes. Due to the low specificity of the anti–P-cadherin antibody used in the cell-culture model, the contribution of this more abundant cell-adhesion protein to podocyte damage can only be speculated. It should also be mentioned that other cell-adhesion molecules of podocytes, such as FAT1 or nephrin, may also be subject to induced ADAM10-mediated shedding and this may also explain the reduced podocyte damage when ADAM10 is missing.[1,2,52] The altered N-cadherin shedding after APN-antibody application led to the idea that a reduced surface expression of cadherins after ADAM10 activation is associated with an increase in the level of intracellular *β*-catenin and, therefore, with an activation of the Wnt signaling pathway.[14,74,75] Such a dysregulated Wnt signaling pathway was already suggested for patients with a predisposition for nephrotic diseases.[20,72] In different murine nephritis models, an increased expression of Wnt ligands have been described,[20,72,76] possibly explaining the contribution of Wnt to the pathology in nephritis. Our observation of an APN-induced and ADAM10-dependent increase in Wnt responsive genes in cultured podocytes, and in the nephritis model, are in support of a regulatory role of the Wnt signaling pathway in mediating podocyte cell adhesion during nephritis.[72] Intriguingly, in control APN littermates, *β*-catenin staining was markedly more intense and widespread in endothelial cells in comparison with the ADAM10*Δ*pod littermates, which might suggest that podocyte ADAM10 could be involved in podocyte-endothelium crosstalk by means of *β*-catenin–induced VEGF regulation[77] in podocytes, which would affect the endothelium.[78]

The pathomechanism(s) of APN-induced ADAM10 activation in podocytes is not yet clear. Cytosolic calcium ion (Ca^{2+}) elevation, as elicitable by treatment of cells with Ca^{2+} ionophores, purinergic receptor agonists, or membrane-perturbing agents,[79,80] is thought to represent the major signaling event to mediate ADAM10 activity through a transient surface exposure to negatively charged phospholipid phosphatidylserine.[81] Whether this mode of ADAM10 activation is relevant in APN-induced podocyte injury requires further investigation; however, elevated Ca^{2+} levels in podocyte injury have been repeatedly reported,[82,83] and purinergic receptor agonists, such as nanobodies to P2X7, have been shown to worsen glomerular injury in the APN model.[84] It also needs to be taken into consideration that the observed activation of the *β*-catenin signaling in our system could be unrelated to ADAM10 activity, and could rather be mediated by secreted factors of the Wnt/*β*-catenin signaling pathway[85,86] and/or the endothelin pathway.[87]

In summary, our study demonstrates a role for ADAM10 activity in driving podocyte injury by shedding of cadherins and by activation of the downstream Wnt/β-catenin pathway. Inhibition of ADAM10 should be considered as a therapeutic option in developing nephritis. However, it needs to be considered that ADAM10 may use a multitude of different substrates[88] and that even subtle alterations of, *e.g.*, Notch signaling after ADAM10 inhibition may affect the therapeutic benefit.

Disclosures

T.B. Huber reports receiving research funding from Amicus Therapeutics and Fresenius Medical Care; having consultancy agreements with AstraZeneca, Bayer, Boehringer-Ingelheim, DaVita, Deerfield, Fresenius Medical Care, GoldfinchBio, Mantrabio, Novartis, and Retrophin; and serving on the editorial board for *Kidney International* and on the advisory board for *Nature Reviews Nephrology*. S.F. Lichtenthaler reports being a scientific advisor for, or member of, *Molecular Neurodegeneration* and receiving research funding from Novartis and Shionogi. T. Wiech reports receiving honoraria from Bayer and Novartis; and being a scientific advisor for, or member of, Retrophin. All remaining authors have nothing to disclose.

Funding

This work was supported by the Deutsche Forschungsgemeinschaft grants ME2108/10-1 (to C. Meyer-Schwesinger), CRC 1192 (project B3 to C. Meyer-Schwesinger and project B8 to T. B. Huber), CRC 877 (project A3 to P. Saftig), Ml1923/1-1 (to P. Saftig), EXC 2145 SyNergy - ID 390857198 (Munich Cluster for Systems Neurology), and FOR2419 (MI 1923/2-1 to P. Saftig). The ERCB-KFB was supported by the Else Kröner-Fresenius-Stiftung.

Data Sharing Statement

The raw data of the files are available at Pride/ProteomExchange (https://www.ebi.ac.uk/pride/archive/login), using the following tokens[89,90]: Dataset, mT/mG dataset; project name, Analysis of Mouse Glomerular Cells; project accession, PXD016238; project DOI, not applicable; username, reviewer50821@ebi.ac.uk; password, UHUYumfS; project name, Murine Glomeruli Membrane Proteomics; project accession, PXD022213; project DOI, not applicable. The reviewer account details are as follows: username, reviewer_pxd022213@ebi.ac.uk; password, AQaw8WEN.

Supplementary Material

Supplemental Data 1:

Acknowledgments

The authors gratefully thank Sonia Wulf, Marlies Rusch, and Anna Berghofer for excellent technical assistance. The authors thank Dr. Desiree Loreth for help in replicate generation for the Immunogold EM, and the Z3 unit of the SFB877.

The authors also thank all participating centers of the ERCB-KFB and their patients for their cooperation.

For active members at the time of the study, please see Shved *et al.*[91]

Dr. S. Wetzel, Dr. J. Reichelt, Dr. W. Sachs, L. Schebsdat, S. Zielinski, Dr. L. Seipold, and Dr. M. Lindenmeyer performed experiments and analyzed data; Dr. T. Wiech selected and provided the human biopsy samples; Dr. C. Meyer-Schwesinger performed confocal microscopy; Dr. S.A. Müller and Dr. S.F. Lichtenthaler performed and L. Heintz analyzed surface proteomics; Dr. O. Kretz and Dr. T.B. Huber performed Immunogold EM; Dr. R. Lüllmann-Rauch performed EM; Dr. S. Wetzel, Dr. C. Meyer-Schwesinger, and Dr. P. Saftig wrote the manuscript; Dr. C. Meyer-Schwesinger and Dr. P. Saftig planned the study.

Footnotes

Published online ahead of print. Publication date available at www.jasn.org.

Supplemental Material

This article contains the following supplemental material online at http://jasn.asnjournals.org/lookup/suppl/doi:10.1681/ASN.2020081213/-/DCSupplemental.

Supplemental Figure 1. Podocyte morphology is preserved in naïve ADAM10Δpod mice.

Supplemental Figure 2. Podocyte morphology is preserved in naïve ADAM10Δpod mice.

Supplemental Figure 3. ADAM10 localization in human glomerular injuries.

Supplemental Figure 4. Glomerular ADAM10 expression increases in APN.

Supplemental Figure 5. Alteration of glomerular morphology is attenuated in APN antibody treated ADAM10Δpod mice.

Supplemental Figure 6. Intrinsic mouse IgG deposition does not differ between ADAM10Δpod and control littermate mice in APN.

Supplemental Figure 7. Alteration of podocyte structure is attenuated in ADAM10Δpod mice in APN.

Supplemental Figure 8. Foot process effacement is attenuated in ADAM10Dpod mice in APN

nephritis.

Supplemental Figure 9. Cultured murine podocytes exposed to APN antibodies represent a suitable model for the analysis of ADAM10 function.

Supplemental Figure 10. The Notch signaling pathway is not activated in an ADAM10-dependent way in podocytes after exposure to APN-antibodies.

Supplemental Figure 11. Activation of Wnt signaling pathways after exposure to APN-antibodies partially depends on ADAM10 in podocytes.

Supplemental Figure 12. N-cadherin is shed in an ADAM10-dependent manner in cultured murine podocytes.

Supplemental Figure 13. Cell-cell adhesion proteins are expressed at the apical side of developing podocytes.

Supplemental Figure 14. P-cadherin expression does not differ between naive ADAM10Δpod and control littermate mice.

Supplemental Figure 15. N-cadherin expression does not differ between naive ADAM10Δpod and control littermate mice.

Supplemental Figure 16.β-Catenin expression is enhanced in the nuclei and cytoplasm of podocytes in the setting of APN nephritis.

Supplemental Table 1. Oligonucleotide sequences for used for qRT-PCR in cultured murine podocytes and isolated glomeruli.

Supplemental Table 2. Summary of the findings regarding ADAM10 regulators in our proteomic datasets.

References

1. Menon MC, Chuang PY, He CJ: The glomerular filtration barrier: Components and crosstalk. *Int J Nephrol* 2012: 749010, 2012. [PMCID: PMC3426247] [PubMed: 22934182]

2. Reiser J, Kriz W, Kretzler M, Mundel P: The glomerular slit diaphragm is a modified adherens junction. *J Am Soc Nephrol* 11: 1–8, 2000. [PubMed: 10616834]

3. Shankland SJ: The podocyte's response to injury: Role in proteinuria and glomerulosclerosis. *Kidney Int* 69: 2131–2147, 2006. [PubMed: 16688120]

4. Matovinović MS: 3. Podocyte injury in glomerular diseases. *EJIFCC* 20: 21–27, 2009. [PMCID: PMC4975266] [PubMed: 27683323]

5. Ronco P, Debiec H: A podocyte view of membranous nephropathy: From Heymann nephritis to the childhood human disease. *Pflugers Arch* 469: 997–1005, 2017. [PubMed: 28597189]

6. Shirato I, Sakai T, Kimura K, Tomino Y, Kriz W: Cytoskeletal changes in podocytes associated with foot process effacement in Masugi nephritis. *Am J Pathol* 148: 1283–1296, 1996. [PMCID: PMC1861509] [PubMed: 8644869]

7. Murphy WM, Moretta FL, Jukkola AF: Epithelial foot-process effacement in patients with proteinuria. *Am J Clin Pathol* 72: 529–532, 1979. [PubMed: 495558]

8. Heymann W, Hackel DB, Harwood S, Wilson SG, Hunter JL: Production of nephrotic syndrome in rats by Freund's adjuvants and rat kidney suspensions. *Proc Soc Exp Biol Med* 100: 660–664, 1959. [PubMed: 13645677]

9. Farquhar MG, Saito A, Kerjaschki D, Orlando RA: The Heymann nephritis antigenic complex: Megalin (gp330) and RAP. *J Am Soc Nephrol* 6: 35–47, 1995. [PubMed: 7579068]

10. Tomas NM, Meyer-Schwesinger C, von Spiegel H, Kotb AM, Zahner G, Hoxha E, et al..: A heterologous model of thrombospondin type 1 domain-containing 7A-associated membranous nephropathy. *J Am Soc Nephrol* 28: 3262–3277, 2017. [PMCID: PMC5661286] [PubMed: 28814510]

11. Meyer-Schwesinger C, Tomas NM, Dehde S, Seifert L, Hermans-Borgmeyer I, Wiech T, et al..: A novel mouse model of phospholipase A2 receptor 1-associated membranous nephropathy mimics podocyte injury in patients. *Kidney Int* 97: 913–919, 2020. [PubMed: 32033781]

12. Meyer-Schwesinger C, Dehde S, Klug P, Becker JU, Mathey S, Arefi K, et al..: Nephrotic syndrome and subepithelial deposits in a mouse model of immune-mediated anti-podocyte glomerulonephritis. *J Immunol* 187: 3218–3229, 2011. [PubMed: 21844386]

13. Meyer TN, Schwesinger C, Wahlefeld J, Dehde S, Kerjaschki D, Becker JU, et al..: A new mouse model of immune-mediated podocyte injury. *Kidney Int* 72: 841–852, 2007. [PubMed: 17653132]

14. Reiss K, Maretzky T, Ludwig A, Tousseyn T, de Strooper B, Hartmann D, et al..: ADAM10 cleavage of N-cadherin and regulation of cell-cell adhesion and beta-catenin nuclear signalling. *EMBO J* 24: 742–752, 2005. [PMCID: PMC549617] [PubMed: 15692570]

15. Maretzky T, Reiss K, Ludwig A, Buchholz J, Scholz F, Proksch E, et al..: ADAM10 mediates E-cadherin shedding and regulates epithelial cell-cell adhesion, migration, and beta-catenin translocation. *Proc Natl Acad Sci U S A* 102: 9182–9187, 2005. [PMCID: PMC1166595] [PubMed: 15958533]

16. van Tetering G, van Diest P, Verlaan I, van der Wall E, Kopan R, Vooijs M: Metalloprotease ADAM10 is required for Notch1 site 2 cleavage. *J Biol Chem* 284: 31018–31027, 2009. [PMCID: PMC2781502] [PubMed: 19726682]

17. Saftig P, Lichtenthaler SF: The alpha secretase ADAM10: A metalloprotease with multiple functions in the brain. *Prog Neurobiol* 135: 1–20, 2015. [PubMed: 26522965]

18. Hartmann D, de Strooper B, Serneels L, Craessaerts K, Herreman A, Annaert W, et al..: The disintegrin/metalloprotease ADAM 10 is essential for Notch signalling but not for alpha-secretase activity in fibroblasts. *Hum Mol Genet* 11: 2615–2624, 2002. [PubMed: 12354787]

19. Niranjan T, Bielesz B, Gruenwald A, Ponda MP, Kopp JB, Thomas DB, et al..: The Notch pathway in podocytes plays a role in the development of glomerular disease. *Nat Med* 14: 290–298, 2008. [PubMed: 18311147]

20. Dai C, Stolz DB, Kiss LP, Monga SP, Holzman LB, Liu Y: Wnt/beta-catenin signaling promotes podocyte dysfunction

and albuminuria. *J Am Soc Nephrol* 20: 1997–2008, 2009. [PMCID: PMC2736766] [PubMed: 19628668]

21. Takemoto M, Asker N, Gerhardt H, Lundkvist A, Johansson BR, Saito Y, et al..: A new method for large scale isolation of kidney glomeruli from mice. *Am J Pathol* 161: 799–805, 2002. [PMCID: PMC1867262] [PubMed: 12213707]

22. Tüshaus J, Müller SA, Kataka ES, Zaucha J, Sebastian Monasor L, Su M, et al..: An optimized quantitative proteomics method establishes the cell type-resolved mouse brain secretome. *EMBO J* 39: e105693, 2020. [PMCID: PMC7560198] [PubMed: 32954517]

23. Wiśniewski JR, Zougman A, Nagaraj N, Mann M: Universal sample preparation method for proteome analysis. *Nat Methods* 6: 359–362, 2009. [PubMed: 19377485]

24. Rappsilber J, Ishihama Y, Mann M: Stop and go extraction tips for matrix-assisted laser desorption/ionization, nanoelectrospray, and LC/MS sample pretreatment in proteomics. *Anal Chem* 75: 663–670, 2003. [PubMed: 12585499]

25. Cox J, Hein MY, Luber CA, Paron I, Nagaraj N, Mann M: Accurate proteome-wide label-free quantification by delayed normalization and maximal peptide ratio extraction, termed MaxLFQ. *Mol Cell Proteomics* 13: 2513–2526, 2014. [PMCID: PMC4159666] [PubMed: 24942700]

26. Hatje FA, Rinschen MM, Wedekind U, Sachs W, Reichelt J, Huber TB, et al..: Tripartite separation of glomerular cell-types and proteomes from reporter-free mice. *bioRxiv.* 10.1101/2020.08.22.262584 (Preprint posted August 22, 2020) [PMCID: PMC8729851] [PubMed: 34074698]

27. Cohen CD, Frach K, Schlöndorff D, Kretzler M: Quantitative gene expression analysis in renal biopsies: A novel protocol for a high-throughput multicenter application. *Kidney Int* 61: 133–140, 2002. [PubMed: 11786093]

28. Cohen CD, Klingenhoff A, Boucherot A, Nitsche A, Henger A, Brunner B, et al..: Comparative promoter analysis allows de novo identification of specialized cell junction-associated proteins. *Proc Natl Acad Sci U S A* 103: 5682–5687, 2006. [PMCID: PMC1421338] [PubMed: 16581909]

29. Tusher VG, Tibshirani R, Chu G: Significance analysis of microarrays applied to the ionizing radiation response. *Proc Natl Acad Sci U S A* 98: 5116–5121, 2001. [PMCID: PMC33173] [PubMed: 11309499]

30. Schiwek D, Endlich N, Holzman L, Holthöfer H, Kriz W, Endlich K: Stable expression of nephrin and localization to cell-cell contacts in novel murine podocyte cell lines. *Kidney Int* 66: 91–101, 2004. [PubMed: 15200416]

31. Althof D, Baehrens D, Watanabe M, Suzuki N, Fakler B, Kulik Á: Inhibitory and excitatory axon terminals share a common nano-architecture of their Cav2.1 (P/Q-type) Ca(2+) channels. *Front Cell Neurosci* 9: 315, 2015. [PMCID: PMC4531237] [PubMed: 26321916]

32. Panzer U, Steinmetz OM, Reinking RR, Meyer TN, Fehr S, Schneider A, et al..: Compartment-specific expression and function of the chemokine IP-10/CXCL10 in a model of renal endothelial microvascular injury. *J Am Soc Nephrol* 17: 454–464, 2006. [PubMed: 16382019]

33. Abramoff MD, Magalhães PJ, Ram SJ: Image Processing with ImageJ. *Biophoton Int* 11: 36–42, 2004.

34. Jorissen E, Prox J, Bernreuther C, Weber S, Schwanbeck R, Serneels L, et al..: The disintegrin/metalloproteinase ADAM10 is essential for the establishment of the brain cortex. *J Neurosci* 30: 4833–4844, 2010. [PMCID: PMC2921981] [PubMed: 20371803]

35. Moeller MJ, Sanden SK, Soofi A, Wiggins RC, Holzman LB: Podocyte-specific expression of Cre recombinase in transgenic mice. *Genesis* 35: 39–42, 2003. [PubMed: 12481297]

36. Weber S, Niessen MT, Prox J, Lüllmann-Rauch R, Schmitz A, Schwanbeck R, et al..: The disintegrin/metalloproteinase Adam10 is essential for epidermal integrity and Notch-mediated signaling. *Development* 138: 495–505, 2011. [PMCID: PMC3014635] [PubMed: 21205794]

37. Farber G, Hurtado R, Loh S, Monette S, Mtui J, Kopan R, et al..: Glomerular endothelial cell maturation depends on ADAM10, a key regulator of Notch signaling. *Angiogenesis* 21: 335–347, 2018. [PMCID: PMC5878725] [PubMed: 29397483]

38. Artavanis-Tsakonas S, Rand MD, Lake RJ: Notch signaling: cell fate control and signal integration in development. *Science* 284: 770–776, 1999. [PubMed: 10221902]

39. Cheng HT, Kopan R: The role of Notch signaling in specification of podocyte and proximal tubules within the developing mouse kidney. *Kidney Int* 68: 1951–1952, 2005. [PubMed: 16221173]

40. Lasagni L, Ballerini L, Angelotti ML, Parente E, Sagrinati C, Mazzinghi B, et al..: Notch activation differentially regulates renal progenitors proliferation and differentiation toward the podocyte lineage in glomerular disorders. *Stem Cells* 28: 1674–1685, 2010. [PMCID: PMC2996085] [PubMed: 20680961]

41. Garg P: A review of podocyte biology. *Am J Nephrol* 47[Suppl 1]: 3–13, 2018. [PubMed: 29852492]

42. Beck LH Jr, Bonegio RG, Lambeau G, Beck DM, Powell DW, Cummins TD, et al..: M-type phospholipase A2 receptor as target antigen in idiopathic membranous nephropathy. *N Engl J Med* 361: 11–21, 2009. [PMCID: PMC2762083] [PubMed: 19571279]

43. Tomas NM, Beck LH Jr, Meyer-Schwesinger C, Seitz-Polski B, Ma H, Zahner G, et al..: Thrombospondin type-1 domain-containing 7A in idiopathic membranous nephropathy. *N Engl J Med* 371: 2277–2287, 2014. [PMCID: PMC4278759] [PubMed: 25394321]

44. Tomas NM, Hoxha E, Reinicke AT, Fester L, Helmchen U, Gerth J, et al..: Autoantibodies against thrombospondin type 1 domain-containing 7A induce membranous nephropathy. *J Clin Invest* 126: 2519–2532, 2016. [PMCID: PMC4922694] [PubMed: 27214550]

45. Doublier S, Ruotsalainen V, Salvidio G, Lupia E, Biancone L, Conaldi PG, et al..: Nephrin redistribution on podocytes is a potential mechanism for proteinuria in patients with primary acquired nephrotic syndrome. *Am J Pathol* 158: 1723–1731, 2001. [PMCID: PMC1891937] [PubMed: 11337370]

46. Wernerson A, Dunér F, Pettersson E, Widholm SM, Berg U, Ruotsalainen V, et al..: Altered ultrastructural distribution of nephrin in minimal change nephrotic syndrome. *Nephrol Dial Transplant* 18: 70–76, 2003. [PubMed: 12480962]

47. Hoettecke N, Ludwig A, Foro S, Schmidt B: Improved synthesis of ADAM10 inhibitor GI254023X. *Neurodegener Dis* 7: 232–238, 2010. [PubMed: 20197648]

48. Hundhausen C, Schulte A, Schulz B, Andrzejewski MG, Schwarz N, von Hundelshausen P, et al..: Regulated shedding of transmembrane chemokines by the disintegrin and metalloproteinase 10 facilitates detachment of adherent leukocytes. *J Immunol* 178: 8064–8072, 2007. [PubMed: 17548644]

49. Reiss K, Bhakdi S: Pore-forming bacterial toxins and antimicrobial peptides as modulators of ADAM function. *Med Microbiol Immunol (Berl)* 201: 419–426, 2012. [PubMed: 22972233]

50. Xu G, Arregui C, Lilien J, Balsamo J: PTP1B modulates the association of beta-catenin with N-cadherin through binding to an adjacent and partially overlapping target site. *J Biol Chem* 277: 49989–49997, 2002. [PubMed: 12377785]

51. Shoval I, Ludwig A, Kalcheim C: Antagonistic roles of full-length N-cadherin and its soluble BMP cleavage product in neural crest delamination. *Development* 134: 491–501, 2007. [PubMed: 17185320]

52. Inoue T, Yaoita E, Kurihara H, Shimizu F, Sakai T, Kobayashi T, et al..: FAT is a component of glomerular slit diaphragms. *Kidney Int* 59: 1003–1012, 2001. [PubMed: 11231355]

53. Wojtalewicz N, Sadeqzadeh E, Weiß JV, Tehrani MM, Klein-Scory S, Hahn S, et al..: A soluble form of the giant cadherin Fat1 is released from pancreatic cancer cells by ADAM10 mediated ectodomain shedding. *PLoS One* 9: e90461, 2014. [PMCID: PMC3953070] [PubMed: 24625754]

54. Reiss K, Maretzky T, Haas IG, Schulte M, Ludwig A, Frank M, et al..: Regulated ADAM10-dependent ectodomain shedding of gamma-protocadherin C3 modulates cell-cell adhesion. *J Biol Chem* 281: 21735–21744, 2006. [PubMed: 16751190]

55. Yaoita E, Nishimura H, Nameta M, Yoshida Y, Takimoto H, Fujinaka H, et al..: Avian podocytes, which lack nephrin, use adherens junction proteins at intercellular junctions. *J Histochem Cytochem* 64: 67–76, 2016. [PMCID: PMC4810789] [PubMed: 26416242]

56. Daugherty RL, Gottardi CJ: Phospho-regulation of Beta-catenin adhesion and signaling functions. *Physiology (Bethesda)* 22: 303–309, 2007. [PMCID: PMC2276853] [PubMed: 17928543]

57. Fagotto F, Funayama N, Gluck U, Gumbiner BM: Binding to cadherins antagonizes the signaling activity of beta-catenin during axis formation in Xenopus. *J Cell Biol* 132: 1105–1114, 1996. [PMCID: PMC2120760] [PubMed: 8601588]

58. Ouyang M, Lu S, Kim T, Chen CE, Seong J, Leckband DE, et al..: N-cadherin regulates spatially polarized signals through distinct p120ctn and β-catenin-dependent signalling pathways. *Nat Commun* 4: 1589, 2013. [PMCID: PMC3602931] [PubMed: 23481397]

59. Seipold L, Altmeppen H, Koudelka T, Tholey A, Kasparek P, Sedlacek R, et al..: *In vivo* regulation of the A disintegrin and metalloproteinase 10 (ADAM10) by the tetraspanin 15. *Cell Mol Life Sci* 75: 3251–3267, 2018. [PMCID: PMC11105247] [PubMed: 29520422]

60. Gutwein P, Schramme A, Abdel-Bakky MS, Doberstein K, Hauser IA, Ludwig A, et al..: ADAM10 is expressed in human podocytes and found in urinary vesicles of patients with glomerular kidney diseases. *J Biomed Sci* 17: 3, 2010. [PMCID: PMC2843607] [PubMed: 20070888]

61. Gutwein P, Abdel-Bakky MS, Schramme A, Doberstein K, Kämpfer-Kolb N, Amann K, et al..: CXCL16 is expressed in podocytes and acts as a scavenger receptor for oxidized low-density lipoprotein. *Am J Pathol* 174: 2061–2072, 2009. [PMCID: PMC2684172] [PubMed: 19435795]

62. Gutwein P, Abdel-Bakky MS, Doberstein K, Schramme A, Beckmann J, Schaefer L, et al..: CXCL16 and oxLDL are induced in the onset of diabetic nephropathy. *J Cell Mol Med* 13[9B]: 3809–3825, 2009. [PMCID: PMC4516529] [PubMed: 19426159]

63. Putaala H, Soininen R, Kilpeläinen P, Wartiovaara J, Tryggvason K: The murine nephrin gene is specifically expressed in kidney, brain and pancreas: Inactivation of the gene leads to massive proteinuria and neonatal death. *Hum Mol Genet* 10: 1–8, 2001. [PubMed: 11136707]

64. Rodewald R, Karnovsky MJ: Porous substructure of the glomerular slit diaphragm in the rat and mouse. *J Cell Biol* 60: 423–433, 1974. [PMCID: PMC2109155] [PubMed: 4204974]

65. Liu G, Kaw B, Kurfis J, Rahmanuddin S, Kanwar YS, Chugh SS: Neph1 and nephrin interaction in the slit diaphragm is

an important determinant of glomerular permeability. *J Clin Invest* 112: 209–221, 2003. [PMCID: PMC164293] [PubMed: 12865409]

66. Quack I, Rump LC, Gerke P, Walther I, Vinke T, Vonend O, et al..: beta-Arrestin2 mediates nephrin endocytosis and impairs slit diaphragm integrity. *Proc Natl Acad Sci U S A* 103: 14110–14115, 2006. [PMCID: PMC1564064] [PubMed: 16968782]

67. Hundhausen C, Misztela D, Berkhout TA, Broadway N, Saftig P, Reiss K, et al..: The disintegrin-like metalloproteinase ADAM10 is involved in constitutive cleavage of CX3CL1 (fractalkine) and regulates CX3CL1-mediated cell-cell adhesion. *Blood* 102: 1186–1195, 2003. [PubMed: 12714508]

68. Abel S, Hundhausen C, Mentlein R, Schulte A, Berkhout TA, Broadway N, et al..: The transmembrane CXC-chemokine ligand 16 is induced by IFN-gamma and TNF-alpha and shed by the activity of the disintegrin-like metalloproteinase ADAM10. *J Immunol* 172: 6362–6372, 2004. [PubMed: 15128827]

69. Yoda M, Kimura T, Tohmonda T, Uchikawa S, Koba T, Takito J, et al..: Dual functions of cell-autonomous and non-cell-autonomous ADAM10 activity in granulopoiesis. *Blood* 118: 6939–6942, 2011. [PubMed: 22042698]

70. Prox J, Bernreuther C, Altmeppen H, Grendel J, Glatzel M, D'Hooge R, et al..: Postnatal disruption of the disintegrin/metalloproteinase ADAM10 in brain causes epileptic seizures, learning deficits, altered spine morphology, and defective synaptic functions. *J Neurosci*. 33: 12915–12928, 12928a, 2013. [PMCID: PMC6619719] [PubMed: 23926248]

71. Tsai YH, VanDussen KL, Sawey ET, Wade AW, Kasper C, Rakshit S, et al..: ADAM10 regulates Notch function in intestinal stem cells of mice. *Gastroenterology* 147: 822–834.e13, 2014. [PMCID: PMC4176890] [PubMed: 25038433]

72. Kato H, Gruenwald A, Suh JH, Miner JH, Barisoni-Thomas L, Taketo MM, et al..: Wnt/β-catenin pathway in podocytes integrates cell adhesion, differentiation, and survival. *J Biol Chem* 286: 26003–26015, 2011. [PMCID: PMC3138306] [PubMed: 21613219]

73. Zavadil J, Cermak L, Soto-Nieves N, Böttinger EP: Integration of TGF-beta/Smad and Jagged1/Notch signalling in epithelial-to-mesenchymal transition. *EMBO J* 23: 1155–1165, 2004. [PMCID: PMC380966] [PubMed: 14976548]

74. Xu L, Corcoran RB, Welsh JW, Pennica D, Levine AJ: WISP-1 is a Wnt-1- and beta-catenin-responsive oncogene. *Genes Dev* 14: 585–595, 2000. [PMCID: PMC316421] [PubMed: 10716946]

75. Taneyhill L, Pennica D: Identification of Wnt responsive genes using a murine mammary epithelial cell line model system. *BMC Dev Biol* 4: 6, 2004. [PMCID: PMC425575] [PubMed: 15140269]

76. Matsui I, Ito T, Kurihara H, Imai E, Ogihara T, Hori M: Snail, a transcriptional regulator, represses nephrin expression in glomerular epithelial cells of nephrotic rats. *Lab Invest* 87: 273–283, 2007. [PubMed: 17260001]

77. Easwaran V, Lee SH, Inge L, Guo L, Goldbeck C, Garrett E, et al..: beta-Catenin regulates vascular endothelial growth factor expression in colon cancer. *Cancer Res* 63: 3145–3153, 2003. [PubMed: 12810642]

78. Dimke H, Maezawa Y, Quaggin SE: Crosstalk in glomerular injury and repair. *Curr Opin Nephrol Hypertens* 24: 231–238, 2015. [PMCID: PMC4465999] [PubMed: 25887901]

79. Maretzky T, Evers A, Le Gall S, Alabi RO, Speck N, Reiss K, et al..: The cytoplasmic domain of a disintegrin and metalloproteinase 10 (ADAM10) regulates its constitutive activity but is dispensable for stimulated ADAM10-dependent shedding. *J Biol Chem* 290: 7416–7425, 2015. [PMCID: PMC4367251] [PubMed: 25605720]

80. Pupovac A, Sluyter R: Roles of extracellular nucleotides and P2 receptors in ectodomain shedding. *Cell Mol Life Sci* 73:

4159–4173, 2016. [PMCID: PMC11108277] [PubMed: 27180276]

81. Bleibaum F, Sommer A, Veit M, Rabe B, Andrä J, Kunzelmann K, et al..: ADAM10 sheddase activation is controlled by cell membrane asymmetry. *J Mol Cell Biol* 11: 979–993, 2019. [PMCID: PMC6927242] [PubMed: 30753537]

82. Burford JL, Villanueva K, Lam L, Riquier-Brison A, Hackl MJ, Pippin J, et al..: Intravital imaging of podocyte calcium in glomerular injury and disease. *J Clin Invest* 124: 2050–2058, 2014. [PMCID: PMC4001540] [PubMed: 24713653]

83. Song N, Yang M, Zhang H, Yang S-K: Intracellular calcium homeostasis and kidney disease [published online ahead of print November 1, 2020]. *Curr Med Chem* 10.2174/0929867327666201102114257 [PubMed: 33138745] [CrossRef: 10.2174/0929867327666201102114257]

84. Danquah W, Meyer-Schwesinger C, Rissiek B, Pinto C, Serracant-Prat A, Amadi M, et al..: Nanobodies that block gating of the P2X7 ion channel ameliorate inflammation. *Sci Transl Med* 8: 366ra162, 2016. [PubMed: 27881823]

85. Schunk SJ, Floege J, Fliser D, Speer T: WNT-β-catenin signalling – a versatile player in kidney injury and repair. *Nat Rev Nephrol* 17: 172–184, 2021. [PubMed: 32989282]

86. Zhou L, Liu Y: Wnt/β-catenin signalling and podocyte dysfunction in proteinuric kidney disease. *Nat Rev Nephrol* 11: 535–545, 2015. [PMCID: PMC4869701] [PubMed: 26055352]

87. Lenoir O, Milon M, Virsolvy A, Hénique C, Schmitt A, Massé JM, et al..: Direct action of endothelin-1 on podocytes promotes diabetic glomerulosclerosis. *J Am Soc Nephrol* 25: 1050–1062, 2014. [PMCID: PMC4005294] [PubMed: 24722437]

88. Kuhn PH, Colombo AV, Schusser B, Dreymueller D, Wetzel S, Schepers U, et al..: Systematic substrate identification indicates a central role for the metalloprotease ADAM10 in axon targeting and synapse function. *eLife* 5: e12748, 2016. [PMCID: PMC4786429] [PubMed: 26802628]

89. Perez-Riverol Y, Csordas A, Bai J, Bernal-Llinares M, Hewapathirana S, Kundu DJ, et al..: The PRIDE database and related tools and resources in 2019: Improving support for quantification data. *Nucleic Acids Res* 47[D1]: D442–D450, 2019. [PMCID: PMC6323896] [PubMed: 30395289]

90. Vizcaíno JA, Csordas A, Del-Toro N, Dianes JA, Griss J, Lavidas I, et al..: 2016 update of the PRIDE database and its related tools [published correction appears in *Nucleic Acids Res* 44: 11033, 2016 10.1093/nar/gkw880]. *Nucleic Acids Res* 44: D447–D456, 2016.

91. Shved N, Warsow G, Eichinger F, Hoogewijs D, Brandt S, Wild P, et al..: Transcriptome-based network analysis reveals renal cell type-specific dysregulation of hypoxia-associated transcripts. *Sci Rep* 7: 8576, 2017. [PMCID: PMC5561250] [PubMed: 28819298]

Figures and Tables

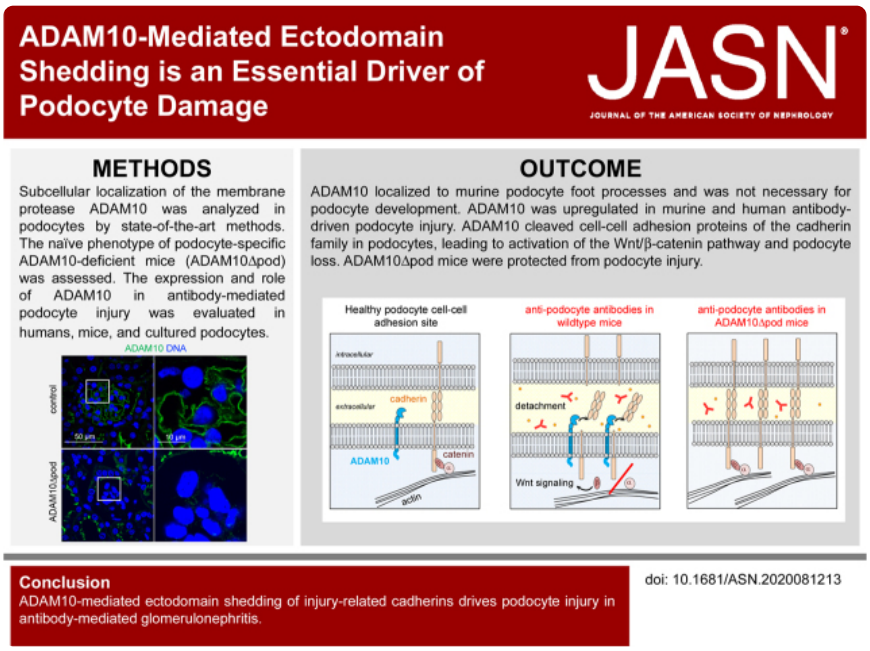

Figure 1.

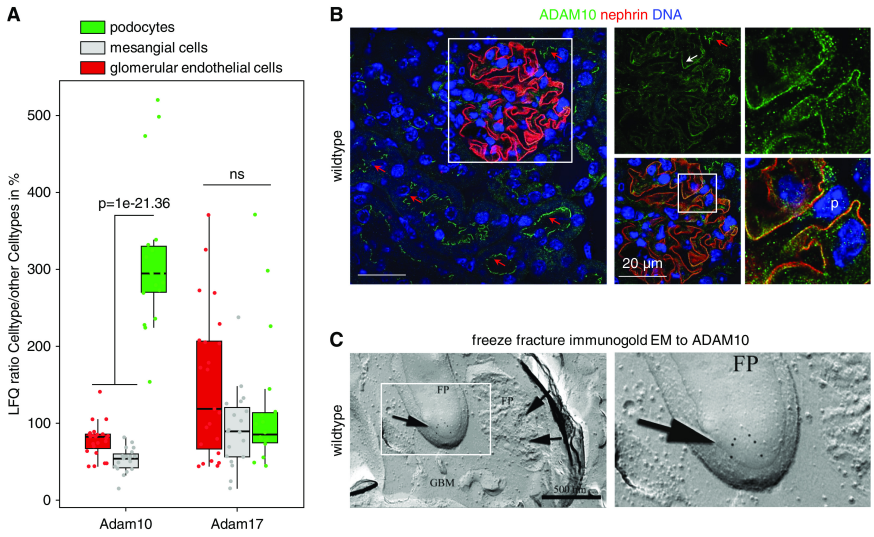

ADAM10 is expressed at podocyte FPs in mice. (A) Proteome analyses of ADAM10 and ADAM17 abundance in FACS-sorted glomerular podocytes and mesangial and endothelial cells. Plotted is the log2 of label-free quantification (LFQ) as percentage difference (*n*=30). (B) Representative confocal images of ADAM10 expression (green) using a rabbit poly-clonal antibody in C57BL/6 glomeruli in relation to the SD protein nephrin (red). DNA is stained in blue (Hoechst). Red arrows point toward apical ADAM10 expression in tubuli; white arrow toward podocyte ADAM10 expression. Colocalization of ADAM10 and nephrin is seen as yellow overlay. (C) Immunogold EM for ADAM10 of glomerular freeze fractures, using a rat mAb to ADAM10, shows specific localization of gold particles at FPs (arrows). GBM, glomerular basement membrane; p, podocyte.

Figure 2.

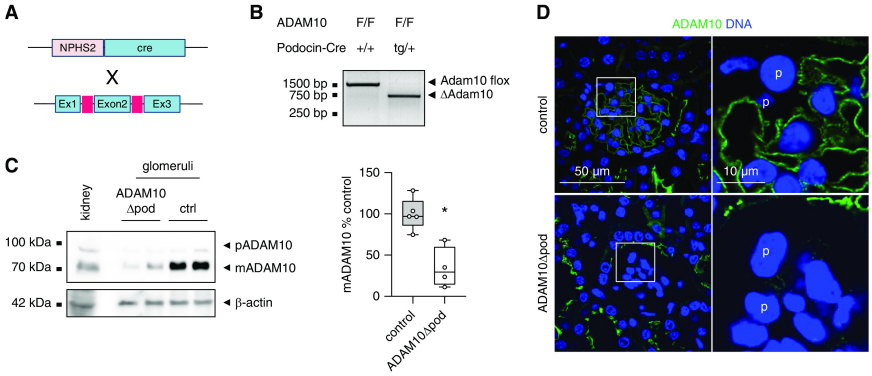

Podocyte-specific deletion of ADAM10. (A) Breeding scheme used to generate podocyte-specific, ADAM10-deficient mice, termed ADAM10Δpod. (B) PCR analysis on isolated glomeruli demonstrates the successful deletion of ADAM10 exon 2 (ΔADAM10) upon Cre expression. (C) Immunoblot from isolated glomeruli reveals reduced ADAM10 abundance in glomeruli of ADAM10Δpod. Total kidney lysate was used as positive control. Graph exhibits densitometric quantification of $n \geq 4$ mice per genotype. *$P \leq 0.05$. (D) Representative confocal image proves specific reduction of ADAM10 (green) in podocytes (p) of naive ADAM10Δpod mice using a rat mAb to ADAM10. +, wild type; ctrl, control; Ex1, exon 1; F, flox; pADAM10, immature ADAM10 proform; mADAM10, mature ADAM10; tg, transgene.

Figure 3.

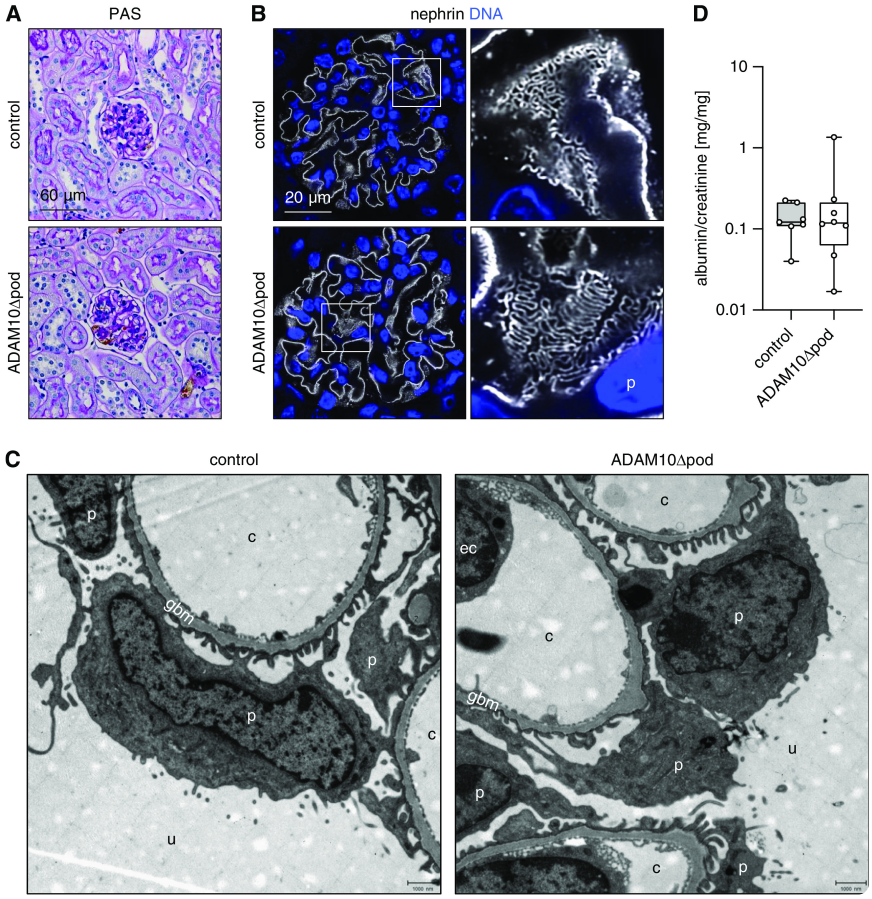

Podocyte development is unaffected by ADAM10 deficiency. Adult ADAM10Δpod and control littermates were compared. (A) Periodic acid–Schiff (PAS) staining of kidney sections exhibiting inconspicuous morphology. (B) Representative high-resolution confocal images of the distribution of nephrin (white) at the SD exhibits a normal, tightly meandering white line in both genotypes. DNA (blue) is visualized by Hoechst staining. (C) EM analysis demonstrates normal podocyte (p) and GFB ultrastructure. Scale bars, 1 μm. (D) Assessment of proteinuria (albumin-creatinine ratio) in urine shows no interference with podocyte function. Pooled data from two independent experiments, $n \geq 7$ per genotype. c, capillary; ec, endothelial cell; u, urinary space.

Figure 4.

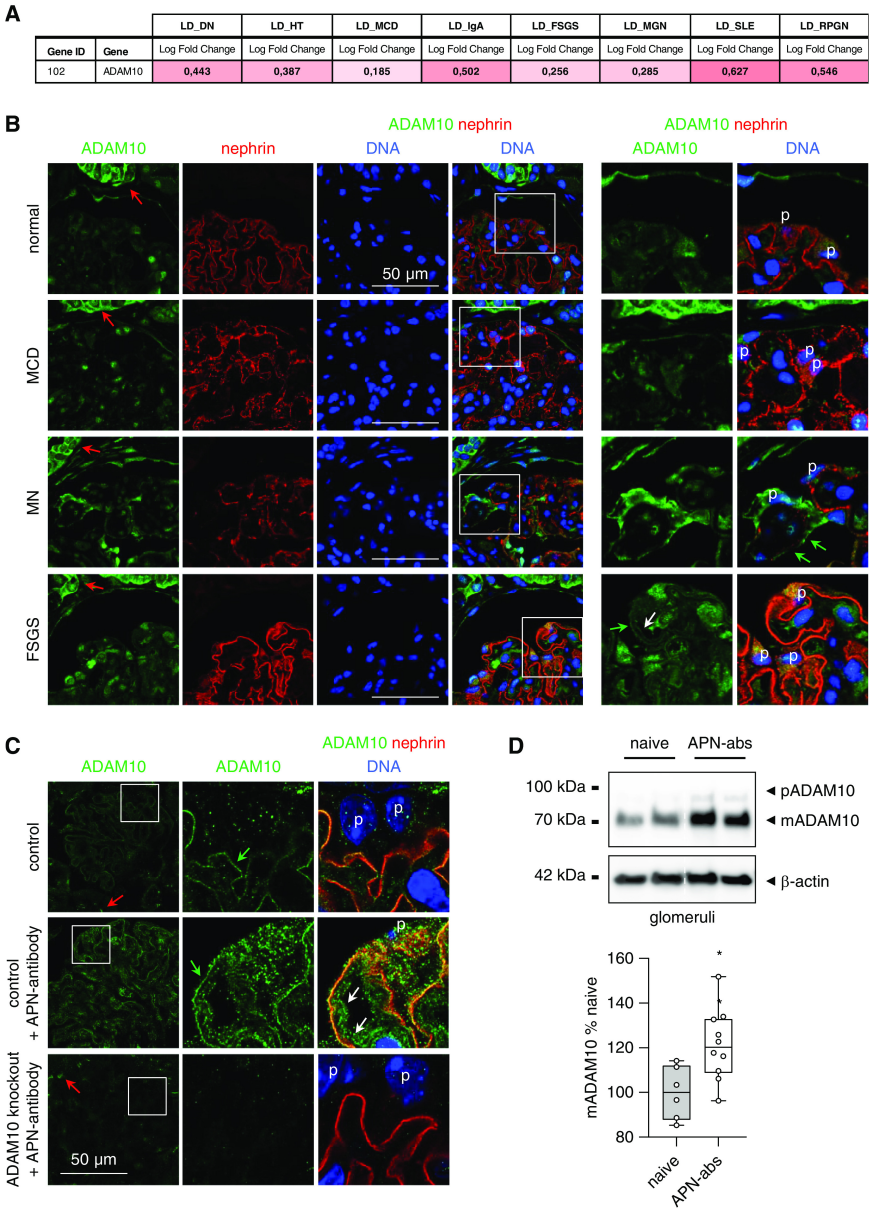

ADAM10 is upregulated in human and murine podocytes upon antibody-mediated injury. (A) Gene expression analysis of ADAM10 mRNA in the glomerular compartment of manually microdissected kidney biopsy specimens from patients with different kidney diseases. Values are expressed as log2 fold change compared with controls (living donors; LD). A *q* value <5% was considered to be statistically significant. (DN, *n*=14; hypertensive nephropathy [HT], *n*=15; MCD, *n*=14; IgA nephropathy [IgA], *n*=27; FSGS, *n*=23; MN [MGN], *n*=21; lupus nephritis [SLE], *n*=32; ANCA-associated GN [RPGN], *n*=23; LD, *n*=42). (B) Representative high-resolution confocal images of ADAM10 (green) expression in human biopsy specimens from patients with nephrotic syndrome due to MCD, MN (PLA_2R1 positive), and FSGS. Note the enhanced podocyte (p) expression in the MN biopsy specimen. Green arrows point toward ADAM10 localization at the podocyte side of the GFB; white arrows toward ADAM10 localization at the endothelial side of the GFB; red arrows toward tubular ADAM10 expression; nephrin shown in red; DNA shown in blue (Hoechst). (C) APN was induced in control littermates and ADAM10Δpod mice. ADAM10 (green) localization was analyzed on day 14 after disease induction. High-resolution confocal images exhibit increased signal for ADAM10 at the podocyte (green arrows) and endothelial cell side (white arrows) of the GFB in APN-treated in comparison with naive control mice. ADAM10Δpod mice show no signal for ADAM10 ex-

pression at the GFB, albeit a preserved tubular ADAM10 expression (red arrows). (D) Immunoblot for ADAM10 levels in isolated glomeruli from naive mice and APN-treated mice on day 14. Graph exhibits densitometric quantification of $n \geq 6$ mice per genotype, pooled data from two independent experiments. *$P \leq 0.05$. Abs, antibodies; mADAM10, mature ADAM10.

Figure 5.

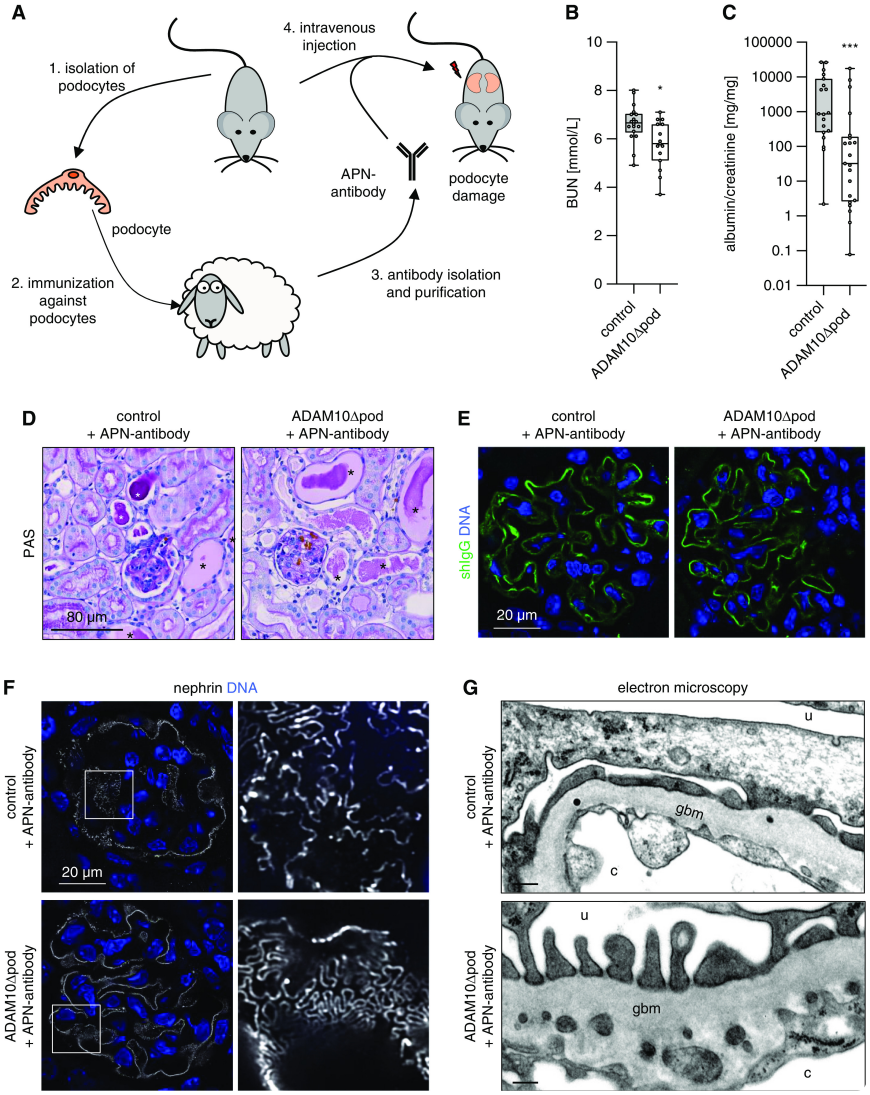

ADAM10 deficiency protects from anti-podocyte antibody–induced podocyte injury. (A) Scheme of the APN model: podocytes are isolated from mouse kidneys (*1*) to immunize sheep (*2*). Sheep-generated, anti-podocyte antibodies are isolated and purified (*3*). APN antibodies intravenously injected into mice bind to podocyte target proteins and induce their injury (*4*). APN was induced in ADAM10Δpod and control littermates. Kidneys were analyzed on day 14 after disease induction. (B) Measurement of BUN levels ($n \geq 15$ per group), $^{*}P \leq 0.05$. (C) Determination of proteinuria (albumin-creatinine ratio) in urine on day 14 reveals decreased development of proteinuria in ADAM10Δpod mice ($n \geq 20$ per group); pooled data from four independent experiments, $^{***}P \leq 0.001$. (D) Representative light micrographs of Periodic acid–Schiff (PAS) staining exhibiting the tubulointerstitial and glomerular morphology. Note the comparable occurrence of PAS-positive protein casts in the tubular lumina (*) of ADAM10Δpod and control littermate mice, contrasting the preserved glomerular morphology in ADAM10Δpod mice. The visible brown, round structures represent the perfused magnetic beads used for glomerular isolation. (E) Confocal analysis of glomerular sheep IgG (green) deposition demonstrates comparable deposition in both genotypes. (F) High-resolution confocal images of the distribution of nephrin (white) at the SD exhibits a strong broadening of the normal, tightly meandering pattern in APN-treated control littermates; whereas ADAM10Δpod showed a mostly preserved pattern. DNA (blue) is visualized by Hoechst staining. (G) Ultrastructural analysis of podocytes demonstrates FPE in control mice upon APN-antibody treatment, whereas ADAM10-deficient podocytes are mostly preserved morphologically. Scale bars, 500 nm. c, capillary lumen; u, urinary

side.

Figure 6.

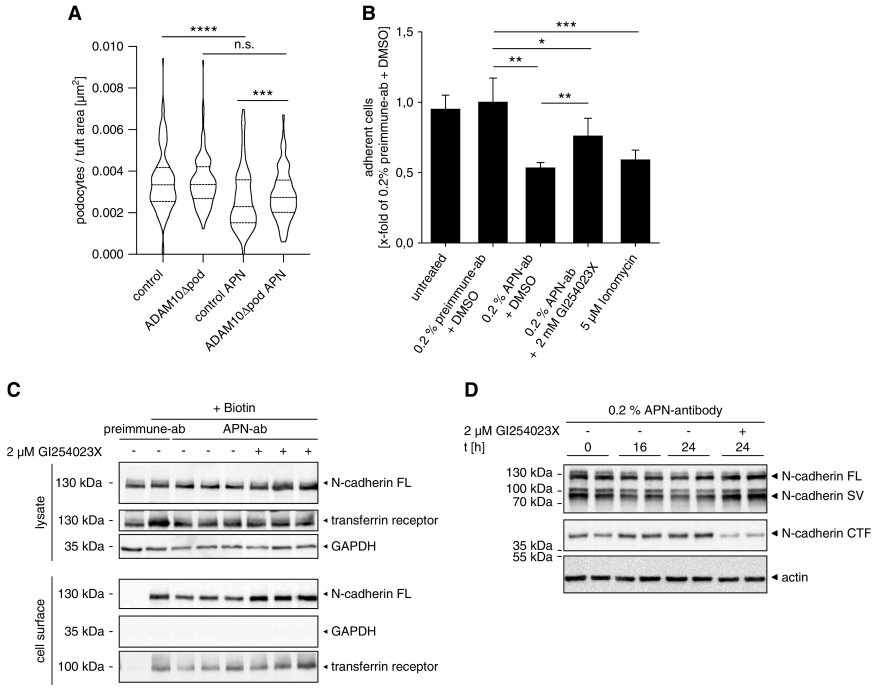

ADAM10-mediated N-cadherin shedding is essential for APN antibody–induced podocyte injury. (A) Quantification of podocyte number per glomerular tuft area in naive and APN-treated ADAM10Δpod and control littermates. Graph exhibits violin plot of pooled data from four independent experiments ($n \geq 12$ per group). (B) Adhesion assay demonstrates APN antibody–induced murine podocyte detachment from the culture dish, which could be suppressed by an ADAM10 inhibitor. The ADAM10 activator ionomycin served as the positive control. One representative out of three individual experiments is shown, each with six replicates per condition. (C) APN antibody (ab) reduces N-cadherin cell-surface levels from murine podocytes, which was rescued by administration of ADAM10 inhibitor GI254023X. The cell-surface protein transferrin receptor and soluble glyceraldehyde-3-phosphate dehydrogenase (GAPDH) served as control for loading and purity of cell-surface extracts. One representative out of three experiments is shown. (D) N-cadherin shedding is increased in response to APN antibody in cultured murine podocytes. ADAM10 inhibition with GI254023X suppressed generation of N-cadherin CTF ($n=4$). In parallel, podocytes were treated with 1 μM DAPT to stabilize the generated N-cadherin CTF. Splice variant (SV) based on the murine protein information at uniprot.org/uniprot/P15116#ptm_processing and uniprot.org/uniprot/D3YYT0#sequences. *$P \leq 0.05$, **$P \leq 0.01$, ***$P \leq 0.001$, ****$P \leq 0.0001$.

Figure 7.

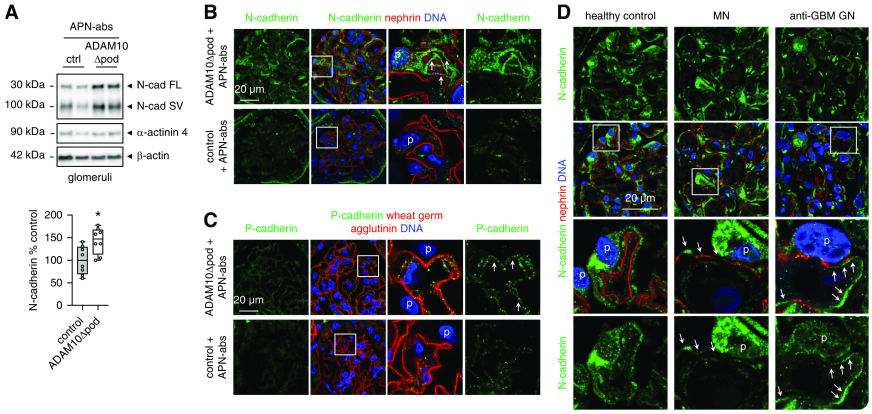

ADAM10 deficiency results in enhanced cadherin levels on podocytes in APN antibody–induced podocyte injury. APN was induced in ADAM10Δpod and control (ctrl) littermate mice, and kidneys were analyzed on day 14. (A) Immunoblot for the cell-cell adhesion molecule N-cadherin (N-cad) levels in isolated glomeruli. Graph exhibits densitometric quantification of n=8 mice per genotype; pooled data from two independent experiments. *P≤0.05. The levels of α-actinin 4 within respective glomerular lysates suggest comparable amounts of podocytes. Splice variant (SV) based on the murine protein information at uniprot.org/uniprot/P15116#ptm_processing and uniprot.org/uniprot/D3YYT0#sequences. (B) Kidneys of mice with comparable mild proteinuria were stained for N-cadherin (green) in relation to the SD protein nephrin (red), and DNA (Hoechst, blue). Note the enhanced expression of N-cadherin in ADAM10Δpod podocytes (p) in comparison to control podocytes. White arrows point toward N-cadherin in presumably primary podocyte processes. (C) Representative confocal images demonstrate enhanced P-cadherin (green) in ADAM10Δpod podocytes in comparison to control podocytes; lectin wheat germ agglutinin (red) visualizes the GFB; DNA (Draq5) shown in blue. Care was taken to use N- and P-cadherin antibodies (Abs) raised in rabbit, so that secondary antibodies needed for visualization would not crossreact with the injected sheep IgG and the intrinsic mouse IgG. (D) Representative confocal images demonstrate podocyte N-cadherin localization in patients with MN and in anti-GBM GN in relation to nephrin (red) and DNA (Hoechst; blue). White arrows represent N-cadherin expression at the podocyte aspect of the GFB, especially in areas where nephrin is absent.

Figure 8.

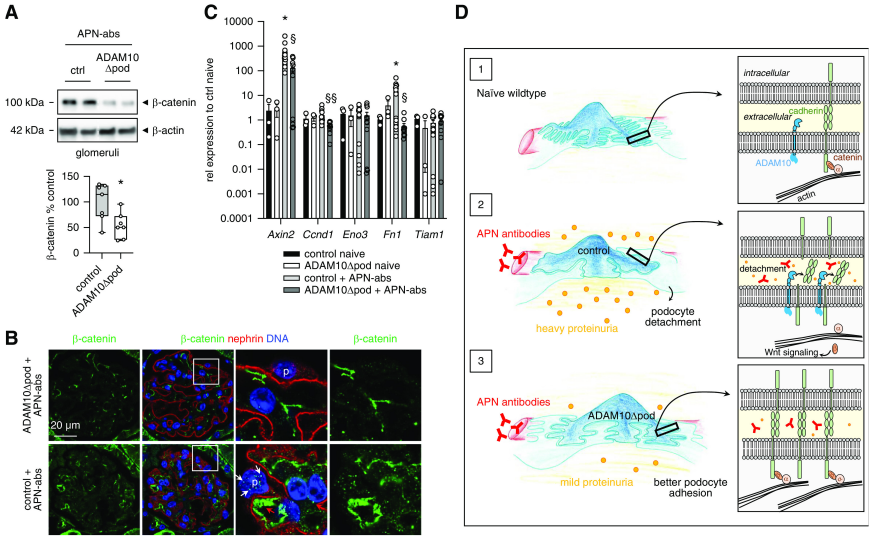

β-Catenin/Wnt signaling pathway is not activated in ADAM10*Δ*pod mice exposed to APN antibodies. APN was induced in ADAM10*Δ*pod and control littermate mice, and kidneys were analyzed on day 14. (A) Immunoblot for *β*-catenin levels in isolated glomeruli. Graph exhibits densitometric quantification of *n*=7 mice per genotype; pooled data from two independent experiments. **P*≤0.05. (B) Kidneys of mice with comparable, mild proteinuria were stained for *β*-catenin (green) in relation to the SD protein nephrin (red), and DNA (Hoechst; blue). Note the enhanced *β*-catenin signal in nuclei (white arrows) and cytoplasm of podocytes (p) and in endothelial cells (red arrow). (C) qRT-PCR analyses of Wnt response genes in isolated glomeruli. Values are depicted as relative expression to naive control (ctrl) littermates after normalization to 18S as housekeeper gene; *n*=3–14 mice per genotype; pooled data from two independent experiments. **P*≤0.05 to control naive, § *P*≤0.05 and §§ *P*≤0.01 to control and APN antibodies (Abs). (D) Scheme depicting proposed role of ADAM10 in podocytes in antibody-mediated podocyte injury. (*1*) Following a prominent embryonic expression of cell-cell adhesion molecules, such as P- and N-cadherin, in podocyte progenitors, healthy mature podocytes have low levels of cadherins at processes. (*2*) In the course of antibody-mediated injury, ADAM10 expression is enhanced. ADAM10 activity results in ectodomain shedding of cadherins. Cadherin cleavage results in a dissociation of *β*-catenin from the cytoplasmic cadherin domain and to a redistribution of *β*-catenin to the cytoplasm and nuclear compartment, where it initiates the transcription of Wnt response genes. Ultimately, this results in decreased cell-cell adhesion and proteinuria. (*3*) As a consequence of loss of ADAM10 activity, cadherin levels are stabilized at podocyte processes, after antibody-mediated injury. *β*-Catenin remains tethered to the cytoplasmic cadherin domain, and the Wnt/*β*-catenin signaling pathway is not activated. Podocyte adhesion is ameliorated, resulting in attenuated proteinuria. ADAM10*Δ*pod, podocyte-specific ADAM10 deletion.